DESIGN AND PREPARATION OF

DNA-ENABLED HYDROGELS

by

Karolyn S. Barker, B.S.

A thesis submitted to the Graduate Council of
Texas State University in partial fulfillment
of the requirements for the degree of
Master of Science
with a Major in Chemistry
May 2016

Committee Members:

Tania Betancourt, Chair

William Brittain

Chad Booth

Kevin Lewis

FAIR USE AND AUTHOR'S PERMISSION STATEMENT

Fair Use

Duplication Permission

DEDICATION

This thesis is dedicated to Christopher Belden and Adam Slinkard, who dared to face cancer undaunted and unflinching, and in doing so showed me the indomitable human spirit that exists within us all.

ACKNOWLEDGEMENTS

I would like to thank my research advisor, Dr. Tania Betancourt, for her guidance and constant support throughout the pursuit of my M.S. degree. Dr. Betancourt has served as a mentor and an inspiration. I have been pushed beyond what I believed to be my capabilities and have accomplished more than I ever could have imagined. The opportunities I have had, as well as all the knowledge I have gained through research in Dr. Betancourt's lab, have guided me to the trajectory of my future in science. Thank you so much, Dr. Betancourt. I know I can speak for the whole lab when I say that we are all incredibly thankful and fortunate to have a boss that we love spending time with in and outside of the lab.

I would also like to thank Dr. William Brittain, Dr. Chad Booth, and Dr. Kevin Lewis for taking the time to be on my committee and providing valuable feedback and support throughout the progress of this thesis. I am also incredibly grateful for all the help that Dr. Shiva Rastogi has provided me. This research would not have been possible without Dr. Rastogi's help synthesizing the precursor molecule used throughout this thesis. Additionally, I would like to thank Dr. Todd Hudnall for being a wonderful professor throughout my graduate studies, as he has always been willing to teach and challenge me, even when I was not enrolled as his student.

When I started research in Dr. Betancourt's lab, I never envisioned that my lab members would ultimately become some of my closest friends. I would like to thank Joe

Dominguez for his many contributions to this thesis, as well as his radiating presence that never fails to brighten my day. I would also like to thank Travis Cantu and Kyle Walsh, who make coming to lab incredibly enjoyable and have become two of my close friends. I am also very grateful for the friendships I have built with Janet Vela Ross, Kelsey Middleton, Tugba Ozel, and Cally Moore. Cally was one of my first friends at Texas State, and has become more than just a friend; she has become family. I could go on for pages about Cally and what a wonderful, brilliant, incredible friend she is. Thank you, Cally, my dodo buddy, I could not have done this without you.

I am incredibly grateful for the education I received from St. Edward's University and the wonderful professors who taught, guided, and motivated me, I would not have realized my potential as a scientist. Dr. Donald Wharry was my research advisor throughout my undergraduate studies. Dr. Wharry is the reason I decided to go to graduate school, as he made me realize that I was the happiest when I was in the lab. I would also like to thank Dr. Henry Altmiller and Dr. Kopecki-Fjetland. St. Edward's is also where I found lifelong friends with a passion for science as deep as mine, Kelly Davis and Anthony Bui.

I would like to thank my family, particularly my mother, whose love and support carried me through not only my graduate studies, but through my entire life. She is my greatest supporter, my greatest motivator, the reason that I believe in myself, and the ultimate role model for the woman I hope to become. My brothers, Kenneth and Nicholas, have been my protectors and I cannot thank them enough for their love and

support. I would also like to thank my dad, stepmom, Nancy, and little sister, Alexa, for their encouragement throughout my education.

Finally, I would like to thank Ted Belden and 1st Lieutenant David Rodriguez. Words will not ever suffice in expressing my gratitude and love for them. Ted has been my foundation and the greatest friend imaginable. He has shaped who I am fundamentally, to the core of my being and I cannot thank him enough. David is the epitome of a leader and has provided me with support and guidance that has always steered me in the right direction. These two men have taught me never to settle and to always do what is right. They have taught me that there is no limit to the things I can accomplish. Thank you Ted and Dave, I love you guys.

TABLE OF CONTENTS

Page

LIST OF TABLES

Table **Page**

LIST OF FIGURES

Figure **Page**

CHAPTER I

INTRODUCTION

Motivation

Most responsive biomaterials that have been developed in recent years rely on the detection and physiochemical response to external or non-specific internal stimuli. Biomaterials that respond to molecules present in a particular environment have not been as extensively explored, which is the focus of the research presented here. For drug delivery, molecular control of material response could be critical to enable drug release at the correct time, dose, and site in the body by delivering cargo only upon interaction with disease-specific molecules. Biomaterials that utilize the functionality of DNA have not been explored significantly. The work herein presented will expand the applicability of DNA aptamers, which are sequence specific strands of RNA or DNA with affinity towards particular molecules. Aptamers will serve to enable biomaterials to be used as molecularly-responsive injectable or implantable scaffolds for drug delivery and other applications.

There is substantial potential for the models presented in this work to serve as versatile hydrogel systems that can be tuned for a variety of applications. The ability to synthesize these hydrogels under conditions similar to those of physiological conditions could allow for encapsulation of living cells, proteins, and drugs within these biodegradable, DNA-based hydrogels.

Overall Research Project

This research project has been approached in a stepwise fashion and is composed of two subprojects to reach the overall goal of designing a molecularly-responsive hydrogel that has potential to be used for drug delivery and other applications by making use of molecules characteristic to a particular environment or diseased tissue. Both subprojects are similar in that they involve the formation of hydrogels utilizing four-arm poly(ethylene glycol) (PEG) as a precursor. All hydrogels within this research utilize DNA as the crosslinking molecule. However, the design of the DNA crosslinker, its response to different molecular stimuli, and the effect of this response on the hydrogel structure is what differentiates the systems developed in each subproject.

Subproject 1

The first project focuses on the design of a hydrogel system crosslinked by single-stranded DNA (ssDNA) that degrades upon interaction with endonucleases.[1] The purpose of this work was to confirm the ability to prepare hydrogels using copper-free click chemistry with DNA as a crosslinking molecule (Figure 1A). It was demonstrated that hydrogel degradation occurs upon exposure to endonucleases DNase I and Benzonase.[1] This project also demonstrated the hydrogel's ability to release cargo encapsulated within the porous network inherent to hydrogels.[1]

Specific aims of subproject 1

1. **Prepare ssDNA-crosslinked PEG hydrogel via click chemistry.** Demonstrate ability to use copper-free click chemistry to form hydrogels with ssDNA crosslinker under physiologically suitable conditions.
2. **Show target-controlled degradability of the hydrogels.** Monitor ability of hydrogels to degrade upon exposure to endonuclease-containing solutions at physiologically relevant concentrations.
3. **Demonstrate encapsulation and release capabilities**. Encapsulate a model protein in order to demonstrate the ability of the hydrogel to hold molecules in the porous network and release them when degraded.

1.2.3 Subproject 2

The second system explores the applicability of aptamers. This project was done in order to demonstrate that a double-stranded DNA (dsDNA) complex containing a relatively well-understood aptamer could serve as a hydrogel crosslinking moiety. The inclusion of an aptamer can elicit degradation of the hybridized aptamer complex (i.e., of the crosslink) in response to preferential binding of the aptamer strand to its target molecule and consequent competitive disruption of the original hybridized complex. Specifically, in this second part of this project, the aptamer specific to the molecule adenosine was hybridized to two DNA strands to serve as the crosslinkers (Figure 1B). This crosslinking is intact when the strands are hybridized, but when adenosine is present in the environment, the preferential binding of the aptamer DNA strand to the adenosine molecule causes dehybridization of the crosslinker complex resulting in degradation of

the hydrogel.

1.2.4 Specific aims of subproject 2

1. **Prepare dsDNA crosslinked PEG hydrogels with adenosine aptamer.** Show ability to use two different methods of hydrogel formation: (1) click-driven and (2) hybridization-driven formation.

2. **Demonstrate hydrogel response to adenosine.** Show that the aptamer complex-crosslinked hydrogels degrade upon exposure to the aptamer's target adenosine.

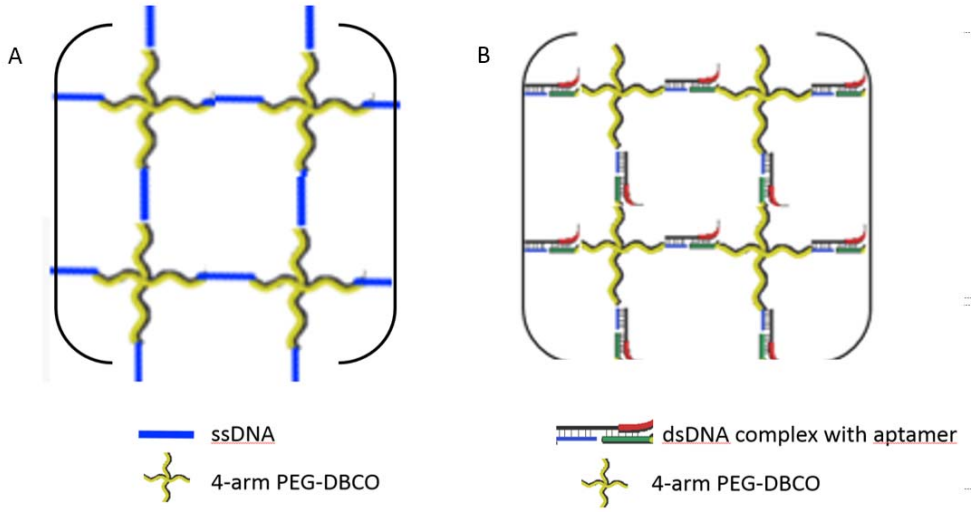

Figure 1. Project Design. **(A)** Overall design of hydrogel in subproject 1 with ssDNA serving as the crosslinking molecule. (**B**) Design of hydrogel in subproject 2 with a dsDNA complex as the crosslinking moiety.

CHAPTER II

BACKGROUND

Hydrogels

Hydrogels are a network of hydrophilic or amphiphilic polymers.[1] The crosslinking of hydrogels can be chemical, physical, or both in nature.[1] Physical hydrogels can be disrupted by physical factors and, therefore, their association is reversible. These physical factors can include environmental stimuli such as pH, temperature, concentration, or ionic strength.[2] Hydrogels that respond to these types of environmental stimuli are discussed below. Chemical hydrogels differ from physical hydrogels in that they are covalently crosslinked and therefore irreversibly associated unless they are chemically degraded via hydrolysis or enzymatic cleavage.[3]

The crosslinked network architecture of hydrogels causes them to be inherently porous. These pores can be used for the encapsulation of a variety of molecules, such as proteins, drugs, DNA, or other biomolecules, depending on the application. Due to this porosity and hydrophilicity, hydrogels are able to readily take up and hold water, thereby swelling. The size of the pores must be taken into consideration when encapsulating agents within a hydrogel. Pore size can be controlled by changing the molecular weight of the polymeric precursors used, adjusting the extent of crosslinking by manipulation of the molar ratios of precursors, or adjusting precursor solution concentrations.

The mechanical properties and hydrophilicity of hydrogels are similar in nature to soft tissues in the body.[4] Because of this, hydrogels have been investigated in a variety of applications in biomedicine. Some of these applications include tissue engineering, cell scaffolds, drug delivery, and biosensing.[5] The function of the hydrogels presented in this

work is demonstrated through their use as drug delivery systems.

Poly(ethylene glycol)

The hydrogels discussed in this work use poly(ethylene glycol) (PEG) as the backbone of the hydrogel. Multi-arm PEGs were crosslinked into hydrogel networks using single or double-stranded DNA (ssDNA or dsDNA) as a crosslinker, as will be detailed in Sections 4.2 and 5.5. PEG is an ideal polymer choice due it being biocompatible and very hydrophilic.[6] PEG is not only soluble in aqueous solutions but also in organic solvents, thereby allowing for facile chemical modification.[7] Because of the hydrophilicity of PEG, it is often a polymer of choice when designing drug conjugates. When PEG is conjugated to a drug that is hydrophobic, it increases its hydrophilicity and solubility, and therefore can allow for increased efficacy and decrease possible aggregation that hydrophobic drugs without conjugation can be susceptible to.[8] In addition, attachment of PEG can reduce immunogenicity, increase stability, and enable longer circulation times.[7]

There are a number of drug delivery systems and drug conjugates utilizing PEG that have been approved by the Food and Drug Administration (FDA) in the United States for a variety of applications.[9] For example, the cancer therapeutic agent Doxil is an FDA-approved PEGylated liposomal doxorubicin formulation that is used to treat breast and ovarian cancers.[7] This is one of the earliest examples showing the therapeutic benefits of PEG, as well as its biocompatibility. There are many other PEG-containing drug delivery systems that have since been approved by the FDA, such as Adagen, Oncaspar, and Somavert.[8,10]

Active and passive drug delivery

Drug delivery can either be accomplished through active targeting or passive targeting. In active targeting, a drug or drug delivery system is generally functionalized with ligands capable of recognizing molecular targets such as antibodies or aptamers. Generally, the ligand meets and forms a complex with a cell that has receptors specific to that ligand, allowing for delivery of the drug to a specific location. The recognition that causes this binding is what differentiates active targeting from passive targeting.

Passive drug delivery employs systems such as micelles, nanoparticles, liposomes, and hydrogels. In passive targeting, the physiochemical properties of these drug carriers can be modified in order to preferentially deliver the drug to a target tissue while avoiding premature metabolism or excretion through natural defense mechanisms of the body.[11] Modifications can include size and molecular weight, pH sensitivity, hydrophilicity, or charge.

In certain cases, the delivery of drugs can be induced molecularly through the use of such biorecognition molecules as DNA aptamers that bind only to particular molecules. Aptamers can be chosen such that they target molecules that are characteristic of or in abundance in the environment where drug delivery is desired. This work specifically focuses on developing a biomaterial that utilizes biorecognitive aptamers as structural components that also enable target-controlled biodegradation and drug release.

Aptamers and Antibodies

Aptamers are specific single-stranded nucleic acid sequences with the ability to bind selectively to particular molecules.[12–14] Although the applications of aptamers overlap with those of antibodies, there are many advantages to the use of aptamers. Antibodies can be split into two groups, monoclonal and polyclonal, which differ in the way they are produced. Polyclonal antibodies are made by injecting animals like rabbits, goats, or sheep with an antigen that evokes an immune response.[15] Polyclonal antibodies are not specific to detecting one epitope, meaning that they bind to multiple sites (epitopes) on a given molecular target. Monoclonal antibodies specifically bind one epitope on a molecule, thereby providing higher specificity and control. Monoclonal antibodies can be produced in the laboratory through an expensive process involving the use of cell lines called hybridomas. However, this process still involves the use of animals, usually mice. In order to produce hybridomas, a specific antigen is injected into a mouse, an antibody-producing cell line from the mouse's spleen is collected, and its B cells are fused with a tumor cell called a myeloma cell.[16] This process allows for the production of monoclonal antibodies in the lab because the hybridoma cells multiply indefinitely and produce a specific antibody.[17] For applications such as drug delivery, monoclonal antibodies are typically a better choice due to their specificity.[18]

Aptamers are chemically synthesized and are therefore intrinsically less expensive compared to antibodies, which are less reproducible since they are originally produced in a living animal. Because aptamers are nucleic acid sequences, either DNA or RNA, they are not typically recognized by the immune system as foreign agents, while antibodies are immunogenic.[19,20] Aptamers can be generated in large numbers and have targets ranging

from simple inorganic molecules, to large protein complexes, and even entire cells.[21] This versatility cannot be achieved by antibodies because there are instances where toxins or molecules do not elicit a strong immune response and therefore antibodies cannot be identified and collected for these target.[20] In addition, aptamers are much smaller and more stable than the proteins that make antibodies.[22] The function of proteins relies on their structure, which can be sensitive to many environmental changes, leading to irreversible denaturation and loss of function.[19] Aptamers can be readily and specifically functionalized with fluorophores or attachments moieties during chemical synthesis at the specific location desired, such as at either end of the sequence, or internally. Antibody modification is much more random and can result in decreased activity.

Process for Selecting Aptamers

The procedure for selecting aptamer sequences is called systematic evolution of ligands through exponential enrichment (SELEX). The cycle starts with a synthetic random DNA oligonucleotide library comprised of over 10^{15} ssDNA fragment sequences which is used directly in the development of DNA aptamers, while this library has to be transferred to an RNA library for RNA aptamers.[23] The steps of SELEX are repetitive and successive and include selection and amplification. The selection process includes binding, partition, and elution. In the first round of SELEX, the target molecules and library are incubated. Oligonucleotide sequences with appropriate affinity or interaction with the target molecule will bind the target. Oligonucleotides that are unbound are removed through thorough washing processes. The oligonucleotides that are bound are then eluted and amplified using polymerase chain reactions (PCR) or real time

polymerase chain reactions (RT-PCR) to obtain many copies of the sequences that bound the target molecule. The enriched pool of olignocleotide sequences that have shown affinity to the target is now smaller and the process is repeated. Generally, the cycle is repeated between 6 and 20 times until a manageable number of possible target-specific aptamers are found. Sequencing is performed on these possible aptamers in order to determine the sequence of the oligonucleotides that can then be later chemically prepared via solid phase oligonucleotide synthesis.

After the SELEX process, there are binding studies that are then performed with this narrow pool of potential sequences in order to verify the aptamer's selectivity for the target molecule. Additionally, counter-SELEX studies are done, which serve the purpose of eliminating sequences that not only bind the target, but also bind other molecules that are structurally similar.[19] This again confirms the selectivity of the aptamer toward only its target.

Environmentally Responsive Hydrogels

Through the use of polymers with responsive properties, hydrogel systems can be developed that respond to single or combined stimuli, either present in the environment or applied externally, creating stimuli-responsive hydrogels.[1,2,24] Environmental stimuli can include pH, temperature, ionic strength, or enzymatic activity. For example, hydrogels composed of pH sensitive polymers containing acidic functional groups such as carboxylic acids will swell under basic conditions, while those with basic functional groups, like amines, will swell in acidic environments.[25–27] Alternatively, hydrogels that are temperature-responsive are comprised of polymers whose solubility is affected by

temperature changes, such as poly(N-isopropylacrylamide).[28]

Light or magnetic fields are examples of external stimuli that can trigger conformational changes affecting the composition of a hydrogel.[24] One particular molecule that changes conformation in response to ultraviolet light is azobenzene, which can be incorporated into a hydrogel network in order to create a hydrogel with light-responsive properties.[29] Ultrasound waves can also be used to disturb the crosslinking of ionically crosslinked hydrogels. Hydrogels that are implanted in a tumor can serve to release high-dosage bursts of chemotherapy directly into the tumor, eliminating some of the toxic effects to peripheral tissues that occur with other chemotherapeutic approaches. Specifically, this has been shown using ionic crosslinking of divalent cations with alginate to form hydrogels with the chemotherapeutic drug mitoxantrone encapsulated.[30] This crosslinking can be disturbed through the application of ultrasound waves, causing the release of the encapsulated drug in the high-dose pulses that are desired. After application of ultrasound, the crosslinking self-heals and allows for controlled drug release.

DNA-Based Hydrogels

DNA can be incorporated into a hydrogel network by being either physically entrapped or covalently conjugated to the polymer backbones. The DNA strands can serve to crosslink the network of the hydrogel. DNA strands can be incorporated as functional units into a hydrogel in the form of aptamers or a DNAzymes.[12] DNAzymes are nucleic acids of particular sequence and structure that enables them to have catalytic ability toward specific chemical reactions.[5] These chemical reactions can include RNA or

DNA cleavage, ligation, or porphyrin metallation.[5] Because DNAzymes are more stable at high temperatures than enzymes, they can be used in numerous applications including in biosensors.[5] As described previously, aptamers are single-stranded DNA or RNA molecules that specifically recognize and bind particular molecules.

The inclusion of DNA into a hydrogel system can allow the hydrogel to be environmentally responsive. One possible stimulus is temperature.[4,31,32] For instance, one of the early examples of a thermoresponsive DNA-enabled hydrogel was designed from succinimide copolymers, poly(N,N-dimethylacrylamide-co-N- acryloyloxysuccinimide)s, that were coupled with terminally modified-amino-DNA strands.[33] When a complementary DNA strand was added to the solution of copolymers, gelation occurred. By heating the hydrogel above the melting temperature, or the DNA dehybridization temperature, the crosslinking is disrupted and therefore the system transitions from a hydrogel into solution. Additional stimuli that induce the swelling or degradation of DNA hydrogels include pH and the presence of metal ions, that can cause the DNA to become charged, triggering conformational changes by forces such as repulsion.[5] Photoresponsive DNA hydrogels have also been reported. For example, through modification of the backbone of DNA molecules with azobenzene, which isomerizes upon irradiation with UV light, the hybridization of crosslinking DNA strands to their complement can be controlled.[34] DNA hydrogels can also be designed such that they respond to biomolecules, such as enzymes. Xing *et al.* reported an enzymatically responsive DNA hydrogels by including an enzymatic restriction cleavage site into the crosslinking DNA strands.[35] Upon the addition of corresponding restriction enzyme, a gel-to-solution transition occurred.[35]

Conclusions

Overall, the development of hydrogels that are molecularly responsive due to the inclusion of DNA in the hydrogel network could lead to a class of biomaterials that are useful for a variety of applications. Because DNA changes conformations in response to environmental or molecular stimuli, it is an ideal material for the preparation of responsive hydrogels. The biocompatibility of PEG has been shown in a variety of systems, and therefore is the polymer that will serve as the backbone of the hydrogels presented in this work. The following chapters will illustrate the ability to have DNA serve as a crosslinker in hydrogels with a PEG backbone.

CHAPTER III

HYDROGEL SYNTHESIS

Click Chemistry

The concept of "click chemistry" was introduced in 2001 by K.B. Sharpless.[36] Click chemistry refers to reactions that possess certain criteria including that the reactions give high yields, create mild byproducts, and are stereospecific.[36] The conditions for these reactions are also specific in that they must be simple and be performed in either no solvent, or benign solvents that can be easily removed.[36] Click chemistry reactions can be broken down into three categories: nucleophilic opening of spring-loaded rings, cycloaddition reactions, and "protecting group" reactions.[36]

The first type of click chemistry, the nucleophilic opening of spring-loaded rings, is enabled by stable, but highly reactive, intermediates including epoxides and aziridines synthesized through the oxidation of olefins.[36] These high-energy intermediates can participate in S_N2 ring-opening reactions that are reliable, stereospecific, and are usually very regioselective.[36] Nucleophilic opening of three-membered rings results in high product yields with facile isolation of products due to the competing elimination processes being stereoelectronically disfavored.[36]

With cycloaddition reactions involving heteroatoms, two unsaturated reactants can be joined to bring about a very large number of different five- and six-membered heterocycles. The Huisgen dipolar cycloaddition of azides and alkynes are one of the most important concerted click reactions due to the orthogonality of aliphatic azides, i.e., their stability under conditions that are standard in many organic synthesis processes.[36]

Based on reversible carbonyl chemistry, the third type of click chemistry reactions involve "protecting group" reactions with diols and hydroxysulfonamides. Cyclic 1,3-dioxolane rings can be produced in high yields with acid-catalyzed reactions with aldehydes and ketones. The dioxolane is resistant to acidic hydrolysis conditions and therefore is stable under most chemical and physiological conditions.

Overall, click chemistry reactions offer many benefits to a variety of applications, as they are stereospecific and simple to perform. Traditionally, the azide-alkyne cycloaddition reaction is copper catalyzed, which poses a problem for biological applications due to the toxicity of the copper.[37,38] The Bertozzi group sought to expand click chemistry reactions and find a way to avoid the use of metal catalysts so that click chemistry could be used for biological applications.[39–41]

Cu-Free Click Chemistry

The Bertozzi group demonstrated the ability of cyclooctynes to label azides, exploring the use of ring strain present in the cyclooctyne molecules, the smallest of the stable cycloalkynes, to drive the reactions.[40] The first cyclooctyne chosen to explore Cu-free click chemistry was one with an electron-withdrawing difluoromethylene moiety because of its inertness in biological systems, its synthetic accessibility, and because this group does not create an electrophilic Michael acceptor that would be capable of alkylating biological nucleophiles.[40] Therefore, the cyclooctyne had ring-strain, as well as electron-withdrawing groups, to act as rate-enhancing features. This cyclooctyne was found to be stable in aqueous solutions and its stability in the presence of 2-mercaptoethanol suggested that cross-reactions with biological nucleophiles was not an

issue with difluorinated-based reagents.[40]

Additionally, the Bertozzi group showed that the difluorinated cyclooctyne (DIFO) (Figure 2) did not cause toxicity in cells and could be used as an alternative method of activating alkynes for [3+2] cycloaddition with azides.[40] This reaction is described as being bioorthogonal because the functional groups that are required for this reaction will not react with other biologically available functional groups, such as carboxylic acids or amino groups. This bioorthogonality allows for these reactions to be used for applications such as *in vivo* imaging, as well as in other applications discussed below.[40]

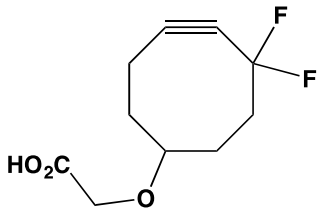

Figure 2. Structure of difluorinated cyclooctyne.

An alternative cyclooctyne, dibenzocyclooctyne (DBCO), is more readily used in Cu-free click chemistry for applications in the areas of biological labeling and biomaterials (Figure 3). Chemistry using DBCO has been used in functionalizing DNA, where the oligonucleotides are modified with DBCO phophoramidite to react with azides via the copper-free strain-promoted alkyne azide cycloaddition (SPAAC) reaction.[42] This work showed that the DBCO group could handle the acidic and oxidative reaction of solid-phase oligonucleotide synthesis, as well as the thermal cycling and conditions of polymerase chain reactions.[42] This is significant because SPAAC on DNA could provide

the ability to functionalize DNA in a simple, selective, and streamlined way.

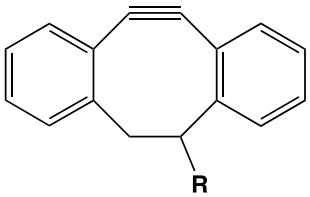

Figure 3. Structure of dibenzocyclooctyne.

The DBCO click reaction has also been used to label sensitive biomolecules with fluorine-18 (^{18}F). Labeling molecules with ^{18}F is a commonly used practice in positron emission tomography (PET), which allows for non-invasive *in vivo* imaging.[43] The aim of this work was to design a ^{18}F-prosthetic group based on DBCO with a triethylene glycol (TEG) spacer to be used as a method for labeling azide-containing biomolecules under less harsh conditions than those traditionally necessary for direct ^{18}F labeling reactions.[43] The labeling of azide-functionalized folate, cRGD peptide, and two peptide mimics of the melanocyte-stimulating hormone (α-MSH) was demonstrated with this methoD.[43] Biomolecule-azides are known for use as tumor targeting vectors, and this work demonstrated superior labeling ability compared to conventional copper-catalyzed click cycloadditions.[43,44]

Additionally, a cyclooctyne-based Cu-free clickable fluorescent probe called fluorescent conjugated DBCO (FC-DBCO) for the intracellular fluorescence labeling of azide-modified biomolecules for specific imaging of live cells has been developed and further demonstrates the applicability of these reactions (Figure 4).[45] This work demonstrated cell membrane permeability of FC-DBCO, which allowed for the

visualization of the intracellular dynamics of azide-mannose and azide-mannoglycoproteins in living HeLa cells.[45] This probe has the potential to be used for applications such as imaging metabolic processes in living cells through the use of azide-modified bioactive small molecules, such as lipids, nucleic acids, and other metabolites, as well as for monitoring drugs and their intracellular dynamics.[45]

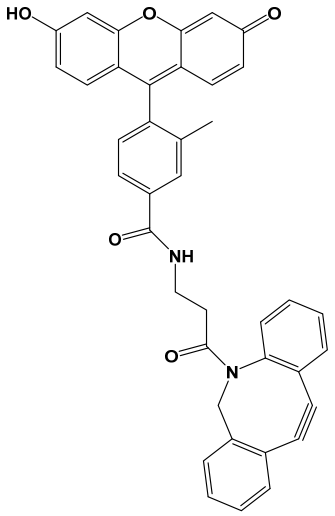

Figure 4. Structure of FC-DBCO.[46]

Copper-free click chemistry using the 1,3-dipolar cycloaddition of azides and cyclooctynes has also been used to label biomolecules in mice, which provides a means of studying biological processes *in vivo*.[39] In a study by Bertozzi *et al.*, mice were injected IP with peracetylated N-azidoacetylmannosamine to label sialic acids on cell-surfaces with azides, followed by subsequent injection with various cyclooctyne reagents.[39] Glycoconjugate labeling was observed in tissues including the intestines, heart, and liver, and no apparent toxicity was observed.[39] Because mice are often used as an animal model to gain understanding into human processes, this work is significant and demonstrates the ability to execute Cu-free click chemistry as a bioorthogonal reaction in

a living system.

The SPAAC is the cu-free click reaction used throughout the work presented in this thesis (Figure 5).[47] This [2+3] cycloaddition relies on the strained dibenzocyclooctyne (DBCO), which has specific reactivity towards azides.[48] The reaction between a DBCO-containing molecule (A) and an azide-containing molecule (B) causes the formation of a triazole ring that links the two molecules together.

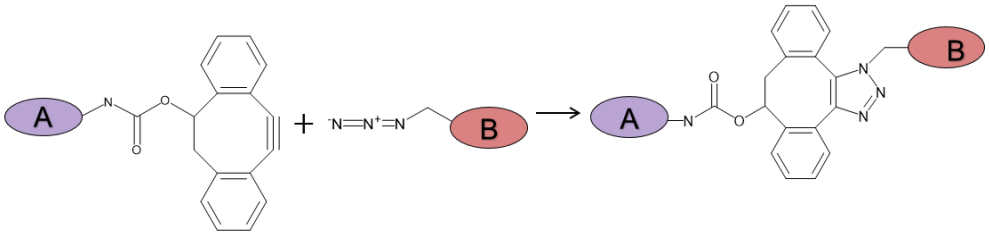

Figure 5. Strain-promoted alkyne-azide cycloaddition.

Synthesis of 4-Arm-PEG-DBCO

Figure 6A shows the chemical schematic for the preparation of 4-Arm-PEG-DBCO, which is used in later steps as a precursor for hydrogel synthesis. Dr. Shiva Rastogi performed this synthesis and gathered the NMR and MALDI-TOF data presented below. Chemical reactions were monitored by thin layer chromatography (TLC) on pre-coated silica gel 60 F_{254} (250 μm) plastic-backed TLC plates (EMD Chemicals Inc.). Visualization was accomplished with UV light. Flash column chromatography was performed on silica gel (32–63 μm, 60 Å pore size). ESI-MS analysis was performed for identification of compound **6** using a Waters Synapt G2 liquid chromatography mass spectrometer (LCMS).

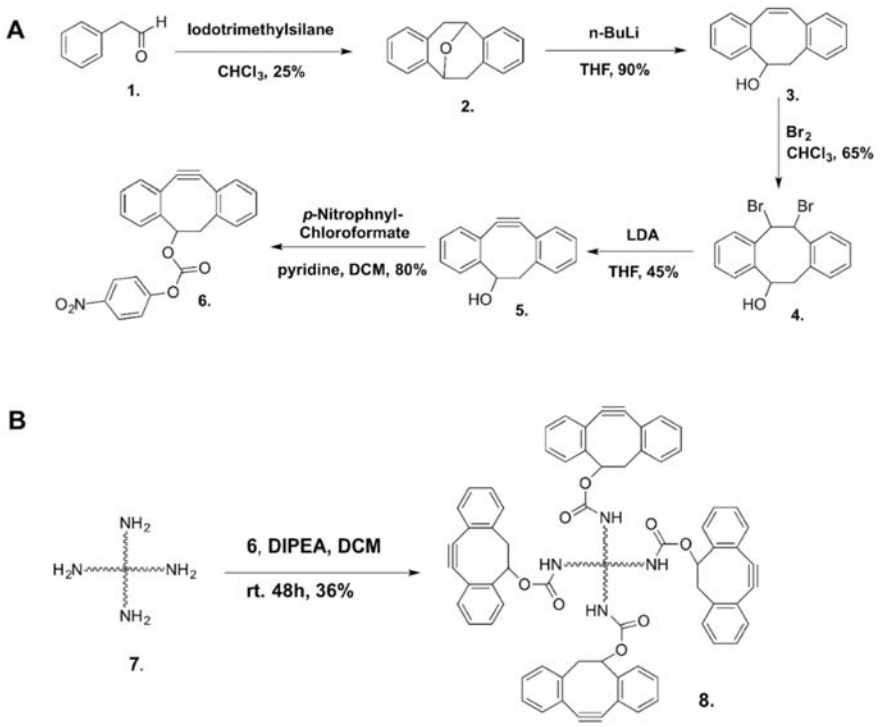

Figure 6. Precursor synthesis scheme. **(A)** Synthesis of para-Nitrophenyl DBCO (Compound **6**, (E)-4-(phenyldiazenyl)phenolic-ester of 5,6-dihydro-11,12- didehydro-dibenzo[a,e] cycloocten-5-yl)**. (B)** Synthesis 4-Arm-PEG-DBCO (Compound **8**).

The carbonic acid, *p*-nitrophenyl ester of 5,6-dihydro-11,12-didehydro-dibenzo[a,e] cycloocten-5-yl, hereon described as *para*-nitrophenyl DBCO (**6**), was prepared as described previously[4] by Dr. Shiva Rastogi in five steps starting from phenylacetaldehyde, as shown in Figure 6A, and characterized by ^{1}H NMR. The NMR spectrum of this product was identical to that reported by Zheng *et al*.[49]

Compound **6** was covalently linked with 4-arm-PEG-NH_2 (M.Wt. 20,000; compound **7**) with a procedure slightly modified from that of Ledin *et al.*, as shown in Figure 6B.[47] To a solution of **7** (200 mg, 0.04 mmol of NH_2) and diisopropylethylamine (DIPEA) (21 μL; 0.12 mmol) in DCM (2 mL), *para*-nitrophenyl DBCO **6** (30.8 mg, 0.08 mmol) was added. The reaction mixture was stirred vigorously at room temperature (rt) for 48 hours under nitrogen atmosphere. The organic solvent was removed under

vacuum. After the synthesis by Dr. Shiva Rastogi, the product was purified in our laboratory by three cycles of dissolution in chloroform followed by precipitation in cold diethyl ether to yield **8** (76.4 mg, 36%).

Characterization of PEG-DBCO

4-Arm-PEG-DBCO was synthesized from 4-Arm-PEG-NH_2 and compound **6** with an overall yield of 36%. This relatively low percent yield is mostly dictated with the purification and recovery product by precipitation, rather than to the synthetic reaction itself.

Figure 7 shows the ^{1}H NMR spectrum of the resulting 4-Arm-PEG-DBCO (compound **8**). ^{1}H was recorded on Bruker 400 (400.13 MHz for ^{1}H; 100.61 MHz for ^{13}C) spectrometer in $CDCl_3$ solvent. Chemical shifts (δ) are reported in ppm relative to the TMS internal standard. Abbreviations are as follows: s (singlet), d (doublet), t (triplet), q (quartet), m (multiplet) and coupling constant (*J*) in Hz. Proton peaks between 7.27 and 7.51 ppm account for the 8 hydrogens on the aromatic rings of the DBCO moiety which are labeled ***a*** on the chemical structure (δ =7.51-7.50 ppm, d, 1H, *J* = 7.3 Hz; 7.36-7.27 ppm, m, 7H). The peaks at 3.18 ppm (dd, 1H, *J* = 15.0, 2.2 Hz, CH_2) and 2.91-2.87 ppm (dd, 1H, *J* = 15.0, 4.0 Hz, CH_2) represent the CH_2 moiety on the octyne ring of DBCO (labeled ***b***). The peak at 5.63 ppm (m, 1H, C*H*O) belongs to the single proton on the carbon connecting the cyclooctyne ring to the PEG chain (labeled ***c***), while that at 5.49 ppm (s, 1H, N*H*) represents the proton on the carbamate bond between PEG and DBCO (labeled ***d***). Finally, the singlet peak at 3.63 ppm (s) of the ^{1}H NMR spectra confirms the presence of the CH_2 groups of PEG (s, 4H, labeled ***e***).

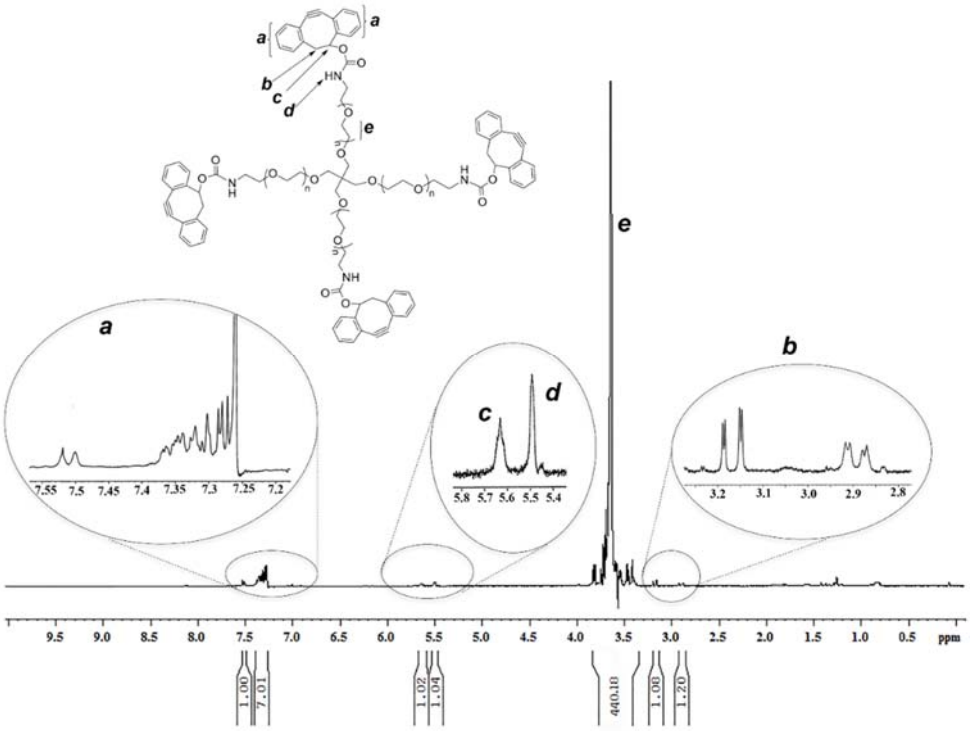

Figure 7. ^{1}H NMR spectrum of the 4-Arm-PEG-DBCO (compound **8**).

The MALDI-TOF spectra for 4-Arm-PEG-NH_2 and the modified 4-Arm-PEG-DBCO are shown in Figure 8. MALDI-TOF MS spectra of compound **7** and 8 was recorded on a Bruker Autflex (TOF/TOF) mass spectrometer using a mixture of 3-hydroxypicolinic acid and ammonium citrate tribasic as a matrix. Samples were desalted with ion exchange resin beads before analysis. A clear increase in the molecular weight of the polymer also indicates successful modification of the polymer with the DBCO moiety.

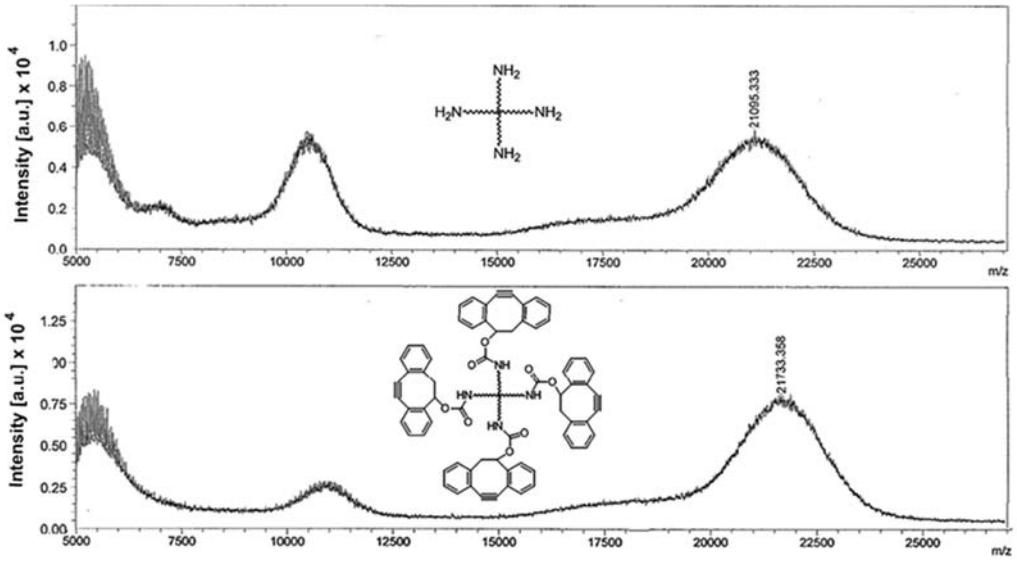

Figure 8. MALDI-TOF spectra of 4-Arm-PEG-NH_2 and the modified 4-Arm PEG-DBCO.

UV-Vis spectroscopy was also used to determine the molar ratio of DBCO to the 4-arm PEG (Figure 9). Absorption spectra of organic compounds were obtained with a Biotek Synergy H4 multi-mode microplate reader in monochromator format. For this purpose, a standard curve of the peak absorption (290 nm) of DBCO alone against concentration was prepared (Figure 9A). An absorbance spectrum of the synthesized 4-arm-PEG-DBCO was then obtained (Figure 9B). The molar ratio of PEG to DBCO was determined using the data from the standard curve to be 3.4 moles of DBCO to every 1 mole of the 4-arm-PEG. This data, together with NMR and MALDI-TOF spectra, indicated that the synthesis of the DBCO-modified PEG precursor was successful.

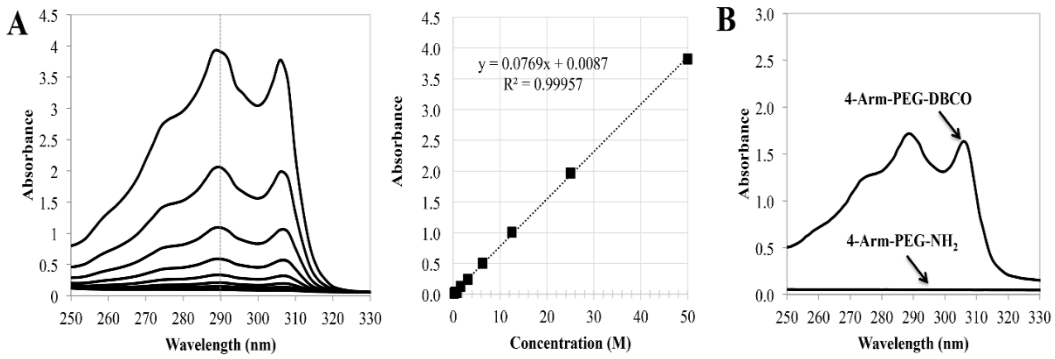

Figure 9. UV-vis characterization. **(A)** Standard curve of the peak absorption (290 nm) of DBCO alone against concentration. **(B)** An absorbance spectrum of the synthesized 4-arm-PEG-DBCO.

Formation of hydrogels using 4-arm-PEG-DBCO and PEG-*bis*-azide

In order to confirm that copper-free click chemistry could be used with the synthesized 4-arm-PEG-DBCO molecules, PEG-*bis*-azide (MW 5,000) was used as a crosslinker. Hydrogels were prepared at room temperature in a 0.01 M phosphate buffered saline (PBS, pH 7.4) by the strain-promoted cycloaddition of 4-arm-PEG-DBCO and azide-functionalized PEG. These two precursor solutions of PEG-*bis*-azide and 4-arm-PEG-DBCO were prepared at a concentration of 0.05 mg/µL and mixed at a molar ratio of 1:2.5. For studies confirming hydrogel formation, specific volumes of the mixed precursor solution were deposited onto a glass microscope slide. The hydrogel precursor solution consisted of 5 w/v% polymer (4-arm-PEG-DBCO and PEG-*bis*-azide). A large-scale hydrogel is shown in Figure 10 to demonstrate that the hydrogel forms as a solid entity.

Figure 10. Macrogel prepared with PEG-*bis*-Azide and 4-arm-PEG-DBCO.

3.3.1 Confirmation of Hydrogel Formation

In order to confirm formation of the hydrogel, a PEG crosslinked hydrogel was prepared as described above. As a control, PEG-*bis*-amine at the same concentration of 0.05 mg/ μL was used instead of PEG-*bis*-azide in the precursor solution with 4-arm-PEG-DBCO. This was used as a control because a hydrogel would not be expected to form without the presence of the azide. Figure 11A shows the PEG hydrogel and the control 15 minutes after the precursor solutions were mixed. The control does not form one entity, but rather appears to crystallize on the surface of the slide (Figure 11A). 15 minutes after the addition of 4 μL of water, the PEG hydrogel swells, while the control appears to go into solution (Figure 11B). Lastly, 50 μL of water was added to the PEG hydrogel and to the control to flood the surrounding area in order to confirm that the hydrogel would not dissolve upon such an excess of water (Figure 11C). The hydrogel is still present after the addition of excess water, while there is no gel apparent with the

control.

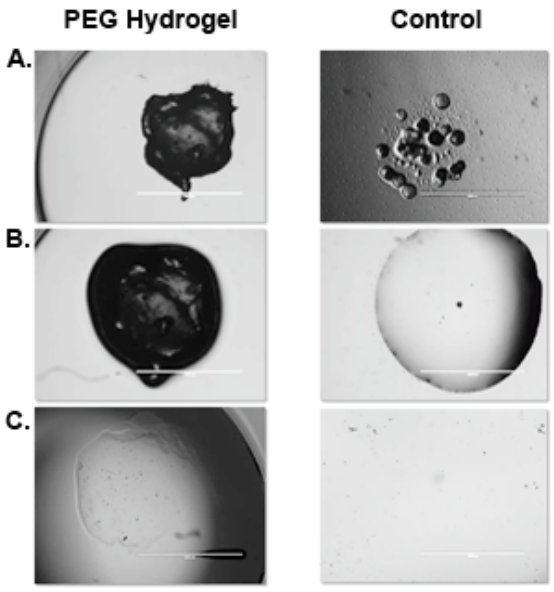

Figure 11. Confirmation of PEG hydrogel. **(A)** Hydrogel and control 15 minutes after plating of precursor solutions. **(B)** 15 minutes after addition of 4 µL of water. **(C)** 15 minutes after an additional 50 µL of water.

3.4 Conclusions

With the method described above, the synthesis of the 4-arm-PEG-DBCO was not only confirmed, but the ability to form hydrogels through the strain-promoted reaction of DBCO and azide groups was too. This was used as a model throughout the rest of the work. Hydrogels prepared using this method were used as a control hydrogels throughout Chapter 4 and Chapter 5. Because they were composed of the non-degradable polyether PEG as a crosslinker, they were used to show that the degradative properties of the hydrogels which contained DNA as a crosslinker (described in Chapters 4 and 5) were due to the presence of DNA, not due to the hydrogel itself.

CHAPTER IV

SINGLE-STRANDED DNA-ENABLED POLY(ETHYLENE GLYCOL) HYDROGELS

Background

In this project, we set out to demonstrate the preparation of DNA-enabled hydrogels that could be degraded by nucleases. Specifically, hydrogels were prepared through the reaction of dibenzocyclooctyne-functionalized multi-arm poly(ethylene glycol) with azide-functionalized single-stranded DNA in aqueous solutions via copper-free click chemistry. Through the use of this method, biodegradable hydrogels were formed at room temperature in buffered saline solutions that mimic physiological conditions, avoiding possible harmful effects associated with other polymerization techniques that can be detrimental to cells or other bioactive molecules. The degradation of these DNA-crosslinked hydrogels upon exposure to the model endonucleases Benzonase and DNase I was studied. In addition, the ability of the hydrogels to act as depots for encapsulation and nuclease-controlled release of a model protein was demonstrated. This model has the potential to be tailored and expanded upon for use in a variety of applications where mild hydrogel preparation techniques and controlled material degradation are necessary including in drug delivery and wound healing systems.

The ability of the hydrogels to encapsulate and act as depots for nuclease-controlled delivery of model therapeutic agents is also demonstrated. There is substantial potential for this model as a versatile system that can be tuned for a variety of applications. The ability to synthesize these hydrogels at physiological conditions could

allow for encapsulation of living cells, proteins, and drugs within these biodegradable, DNA-based hydrogels.

Importance

To date, few reports of the use of the interaction of DNA-enabled biomaterials with nucleases have been reported. Specifically, Li *et al.* demonstrated the use of aptamer-decorated polyacrylamide hydrogels for catch and nuclease-enabled release of circulating tumor cells while Tian *et al.* investigated the potential of DNA-polyethyleneimine microcapsules to release a model protein on interaction with the T7 exonuclease enzyme.[50,51] These accounts demonstrate the potential of this nascent nuclease-dependent release mechanism and encourage further exploration of the applications of DNA-enabled biomaterials.

Endonucleases are critical for mechanisms of DNA repair. However, they are also known to be overexpressed in cancer and to be present in wounds with bacterial contamination. Endonucleases are of great importance in the human body as they are critical for many mechanisms of DNA repair. Variation in the activity and concentration of the endonuclease DNase I can be indicative of disease progression, patient prognosis, and effectiveness of treatment in cancer and other diseases.[52] An example of this can be seen in the early stages of acute myocardial infarction, where it has been found that DNase I activity abruptly increases.[53] Yasuda and colleagues observed that exposure to a hypoxic environment led to a 15-fold upregulation of the DNase I gene transcription in human pancreatic cancer cells.[54] DNase I might be a potential marker for detection and diagnosis of transient myocardial ischemia and other ischemic conditions, and could be

used as a trigger for responsive therapeutic strategies.

An association has been found between patients with gastric and colorectral carcinoma and DNase I phenotype two.[55] Spandidos and colleagues studied the activity of DNases I and II in the serum of both healthy donors and in patients with breast tumors.[56] It was found that in the serum of healthy donors, activity of DNase I varied from 0 to 200 U/mL.[56] In patients with benign tumors, there was an increase in DNase I activity in 3% of all cases.[56] However, in those patients with malignant forms, it was observed that DNase I activity increased in 58% of patients and that those patients with more advanced stages of the disease had the highest DNase I activity.[56] Patients with stage III breast cancer who underwent surgical resection showed a decrease in activity of 92% 21-30 days following the operation.[56]

In addition to DNAse I, the level of expression of other endonucleases such as the flap endonuclease 1 (FEN1) and the apurinic/ apyrimidinic endonuclease (APE1) in cancer has also been studied. Overexpression of these endonucleases is a feature recognized in many types of cancer and such expression can be a prognostic factor.[57] FEN1 is part of the Rad2 structure-specific nuclease family involved in many activities throughout the body and is reported to interact with over thirty proteins from different DNA metabolic pathways.[58] Kaina and colleagues reported overexpression of FEN1 in testis, lung, and brain tumors.[59] Of the 48 various tumor tissue samples analyzed in their studies, 37 had higher expression of FEN1 than normal tissue studied from the same patients. This particular endonuclease has also been found to be overexpressed in lung and gastric cancers.[57] Due to the prevalence of overexpression of nucleases in a variety of cancers, DNA-enabled hydrogels could have potential applications in cancer

therapy where they could be administered via injection and used as drug delivery depot that could be triggered to release therapeutic agents upon interaction with tumor nucleases.

Nucleases, and in particular DNase I, can also pose threats to humans, particularly with regard to wound infections. There are many types of bacteria that are present in infected wounds, with *Staphylococcus aureus* being one of the most common.[60] Shehabi *et al*. investigated isolates of *Staphylococcus aureus* from the nasal cavity and those in wounds.[61] They reported that the only virulence factor produced significantly more in wounds than in the nasal cavity was the endonuclease deoxyribonuclease I (DNase I), which was present in 97.5% of samples studied.[61] The presence of nucleases in wounds has been shown to prolong infection. Nuclease degradable hydrogels could be loaded with therapeutic agents such as antibiotics and used to help treat infections caused by bacteria such as *S. aureus.*

The work presented in this chapter focuses primarily on demonstrating the ability of ssDNA to act as the crosslinking molecule in the hydrogel system, specifically using copper-free click chemistry. The hydrogels discussed in this chapter show the ability to be synthesized in aqueous, benign environments, as well as to controllably degrade and release of encapsulated molecules upon interaction with physiologically relevant nucleases demonstrating their potential functionality in as responsive biomaterials for drug delivery and other biomedical applications.

Experimental

Materials

Single-stranded DNA functionalized on both the 5’ and 3’ ends with azide groups

(N_3−GCTCCGTGCGAGGGTCGAGCCC−N_3, MW 8,658 Da) was obtained from Integrated DNA Technologies (Coralville, IA). Poly(ethylene glycol) bisazide (PEG bisazide, average MW 5,000) and Benzonase® Nuclease (recombinant, expressed in *E.* coli) were purchased from Sigma Aldrich (St. Louis, MO). RNase-free DNase I from bovine pancreas and DNase I buffer were obtained from Life Technologies (Waltham, MA). Phosphate buffer saline (PBS, 0.01 M) was purchased from KPL (Gaithersburg, MD). 4-Arm-PEG terminated in amine groups (4-arm-PEG-NH_2) was obtained from Laysan Bio (Arab, AL). Dry solvents were obtained using a solvent purification system (Innovative Technology, Inc.). Ultrapure water (18.2 ΩM) was obtained from a Millipore Direct-Q3 UV ultrapure water system. All other reagents, solvents, and catalysts were purchased from commercial sources (Acros Organics and Sigma-Aldrich) and used without purification.

Hydrogel Preparation

Hydrogels were prepared at room temperature in 0.01 M phosphate buffered saline (PBS, pH 7.4) via the strain-driven cycloaddition of 4-arm-PEG-DBCO and a DNA crosslinker functionalized with azide groups on both ends. Solutions of 4-Arm-PEG-DBCO and azide-functionalized DNA in PBS at a concentration of 50 μg/μL were mixed at a molar ratio of 1 : 2.5 at room temperature to a final volume of 0.3 μL (0.15 μL of each precursor solution) onto a glass microscope slide. The hydrogel precursor solution consisted of 5 %w/v polymer (4-Arm-PEG-DBCO and azide-functionalized DNA). The precursor solution was covered to prevent drying, and allowed to react for 15 minutes for gelation to occur. As a control, hydrogels were also prepared utilizing

PEG bisazide (MW 5,0000) as a linker instead of azide-functionalized DNA (MW 8,658) at the same molar ratio.

Optical Images of Hydrogels: To demonstrate hydrogel formation, optical images of the hydrogels were taken using a Ramé-Hart Instrument Co. goniometer (Model 200-F1) equipped with an adjustable sample stage, diffuse white light source, and monochromatic digital camera. Hydrogels were prepared as described above but on a silicon wafer substrate. Controls consisted of unreactive precursor solutions consisting of 4-Arm-PEG-NH_2 and either amine-functionalized DNA (NH_2−GCTCCGTGCGAGGGTCGAGCCC−NH_2) or PEG bisazide at the same volume and molar ratios as the samples. Upon a gelation period of 15 minutes, samples were uncovered and images were taken of the hydrogels every minute over a period of 10 minutes as the hydrogels dried. Additional optical images of the hydrogels were obtained with a Nikon D5000 camera.

Scanning Electron Microscopy of Hydrogels: Scanning electron microscopy (SEM) imaging was performed to investigate the internal structure of the hydrogels. Specifically, hydrogels were prepared as described above but on a silicon wafer substrate. The hydrated hydrogels were then frozen in liquid nitrogen and lyophilized using a Labconco FreeZone 4.5 Liter benchtop freeze drying system. The freeze-dried hydrogels were then sputter coated with 2 nm of iridium using an EMS Quorum EMS150T ES turbo-pumped sputter coater. The hydrogels were imaged with a Helios NanoLab 400 - FEI scanning electron microscope at 5 kV and 86 pA.

Quartz Crystal Microbalance: eQCM 10M quartz crystal microbalance (Gamry Instruments, Warminster, PA). The 10 MHz gold-coated quartz

crystal was secured within a liquid Teflon cell (Gamry) and maintained at a temperature of 32 °C.

Nuclease-Mediated Hydrogel Degradation with Benzonase

Hydrogels were degraded by exposure to Benzonase® endonuclease. Enzyme solutions were prepared to a final buffer concentration of 5 U/mL in a PBS solution containing 2 mM $MgCl_2$ at a pH of 8. Enzyme concentration is generally expressed in the number of units per volume. A unit describes the activity of the enzyme or, more specifically, the amount of the enzyme that catalyzes the conversion of 1 micro mole of substrate per minute. A volume of 75 μL of this buffer solution was added to the 0.3-μL hydrogels. Hydrogel degradation was monitored visually via microscopy. Specifically, hydrogels were photographed every 5 minutes over a period of 45 minutes to observe the degradation process. Controls included DNA-crosslinked hydrogels exposed to nuclease-free buffer, and PEG-crosslinked hydrogels exposed to Benzonase® solution at 5 U/mL.

Study of Hydrogel Degradation via Quartz Crystal Microgravimetry

To investigate the degradation of the DNA hydrogels upon interaction with nucleases in a more quantifiable manner, degradation studies were done via quartz crystal microgravimetry. For enzymatic degradation studies, the physiologically relevant nuclease DNase I was utilized. DNA- or PEG-crosslinked hydrogels were prepared as discussed in Section 4.2.2 directly on the center of the quartz crystal, and allowed to react for 15 minutes while covered to prevent dehydration during the gelation process. The

hydrogels were then covered with 200 μL of preheated DNase-free buffer (10 mM Tris, 2.5 mM $MgCl_2$, 0.5 mM $CaCl_2$, pH 7.5, Life Technologies) and the resonant frequency of the crystal was monitored for 60 minutes. The buffer was then removed and replaced with 200 μL of preheated DNase solution (10X concentration = 291 U/mL) and the frequency of the crystal was monitored for 60 additional minutes. Changes in the resonant frequency of the crystal were monitored over time.

Protein Encapsulation and Nuclease-Mediated Release

To demonstrate the ability of the hydrogels to act as depots for encapsulation of therapeutic agents and their potential for nuclease-triggered agent release, hydrogels were prepared in the presence of a model protein. Specifically, bovine serum albumin (BSA) labeled with fluorescein isothiocyanate (FITC) was used as a model protein. BSA-FITC was prepared by dissolving BSA in carbonate buffer, pH 9.0, and reacting with FITC for 4 hours. The BSA-FITC conjugate was purified by dialysis against carbonate buffer and water, followed by lyophilization. Hydrogels were prepared as described in Section 4.2.2 using Labtek™ chambered slides as substrates, but using a 1 mg/mL solution of BSA-FITC instead of water as the dissolving medium. Brightfield and fluorescence images of the hydrogels were obtained using an EVOS FL digital fluorescence microscope. Fluorescence images were obtained using a GFP LED light source/filter cube (λ_{Ex} = 470/22 nm, λ_{Em} = 525/50 nm). Hydrogels were then flooded with 100 μL of nuclease-containing (1X = 29.1 U/mL, 10X = 291 U/mL) or nuclease-free buffer and images were obtained over time to track the release of the fluorescence protein and the hydrogel degradation. In addition, samples of the surrounding medium were

collected at specific time periods for quantification of protein release via fluorescence spectroscopy using a standard curve of BSA-FITC in buffer.

Hydrogel Synthesis and Characterization

Figure 12 shows the proposed mechanism for the preparation of drop-casted DNA-crosslinked hydrogels via copper-free click chemistry, as well as their function as degradable biomaterials in response to endonuclease activity. Hydrogels were prepared by drop casting 4-Arm-PEG-DBCO and crosslinker precursors in PBS buffer (pH 7.4) and allowing them to react at room temperature.

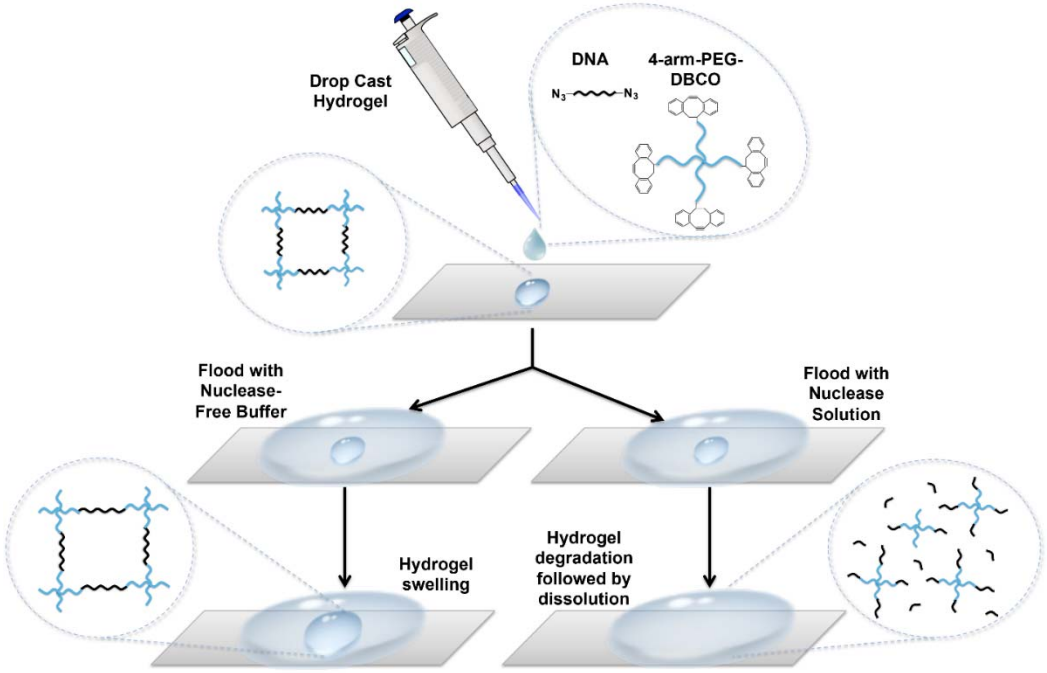

Figure 12. System 1 overview. Hydrogel network formation via copper-free click chemistry, followed by hydrogel swelling when immersed in nuclease-free buffer, or biodegradation when incubated in the presence of nucleases.

Two crosslinker types were used: PEG bisazide (nuclease-resistant control) and DNA bisazide (N_3−GCTCCGTGCGAGGGTCGAGCCC−N_3). Hydrogel gelation occurred for both the PEG-crosslinked control and the DNA-crosslinked sample within

15 minutes.

To confirm hydrogel formation, optical images of the 0.3-μL DNA or PEG-crosslinked hydrogels were obtained using a goniometer system as hydrogels underwent drying at room temperature. The purpose of these studies was to demonstrate the ability of the hydrogels to retain their three-dimensional shape and hydration compared to non-gelating solutions containing the same molar quantity of the unreactive precursors 4-Arm-PEG-NH_2 (instead of 4-Arm-PEG-DBCO) and either DNA or PEG of the same sequence or molecular weight as that used for hydrogel preparation, respectively. As shown in Figure 13, both DNA and PEG-crosslinked hydrogels retained their three-dimensional structure even when dried for 10 minutes, compared to the non-gelating controls that completely collapsed upon drying. This non-traditional optical method was utilized as opposed to more commonly used tilt or rheology methods for demonstration of hydrogel formation because of the small size of the hydrogels herein employed.[62,63] With microscopic samples such as these, high sample surface tension and low gravitational force prevents sample flow regardless of gelation status. On the other hand, rheology studies necessitate samples that are over 20 μL in size which become prohibitory due to the current cost of the azide-derivatized DNA oligonucleotides. It was also demonstrated that the hydrogel can swell but does not dissolve in excess solvent. Hydrogel gelation kinetics could be studied further using microrheology.[64,65]

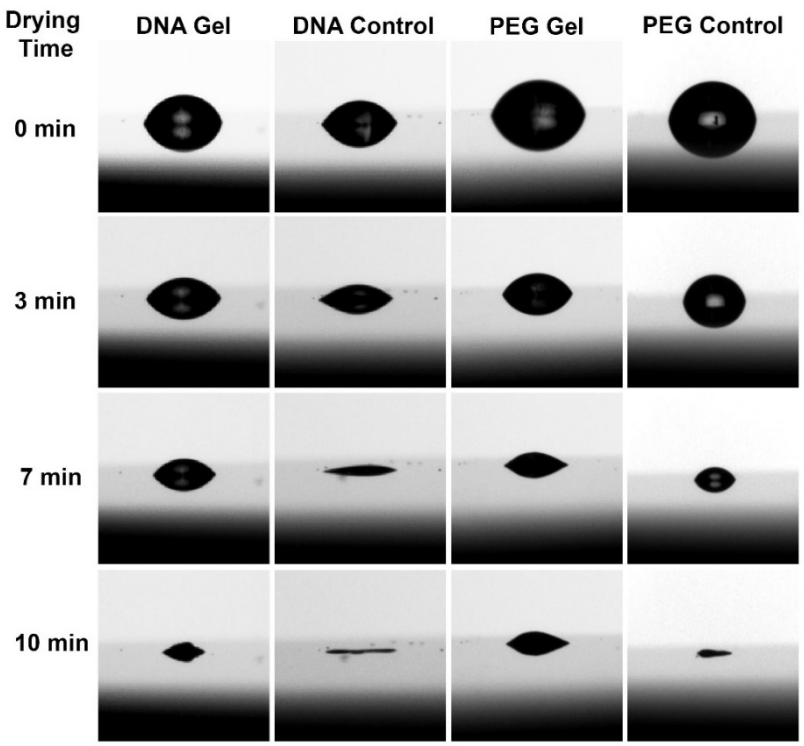

Figure 13. Goniometer images. Images of hydrogels and controls before, during, and after the process of drying at room temperature. DNA and PEG-corsslinked hydrogels were prepared using 4-Arm-PEG-DBCO and either N_3−GCTCCGTGCGAGGGTCGAGCCC−N_3 (DNA Gel) or PEG bisazide (PEG Gel), respectively. DNA and PEG-based controls were prepared with 4-Arm-PEG-NH_2 and NH_2−GCTCCGTGCGAGGGTCGAGCCC−NH_2 (DNA Control) or PEG bisazide (PEG Control) at the same molar concentration as the samples. Both controls collapse within this time period while the hydrogels retain their three-dimensional structure.

Figure 14 shows scanning electron microscopy images of DNA- and PEG-crosslinked hydrogels. These images demonstrate that both types of hydrogels have a cellular structure with macropores of approximately 1 μm in diameter. As expected, controls prepared form non-reacting precursors did not form porous cellular structures but instead collapsed into undefined films (Figure 14G-I).

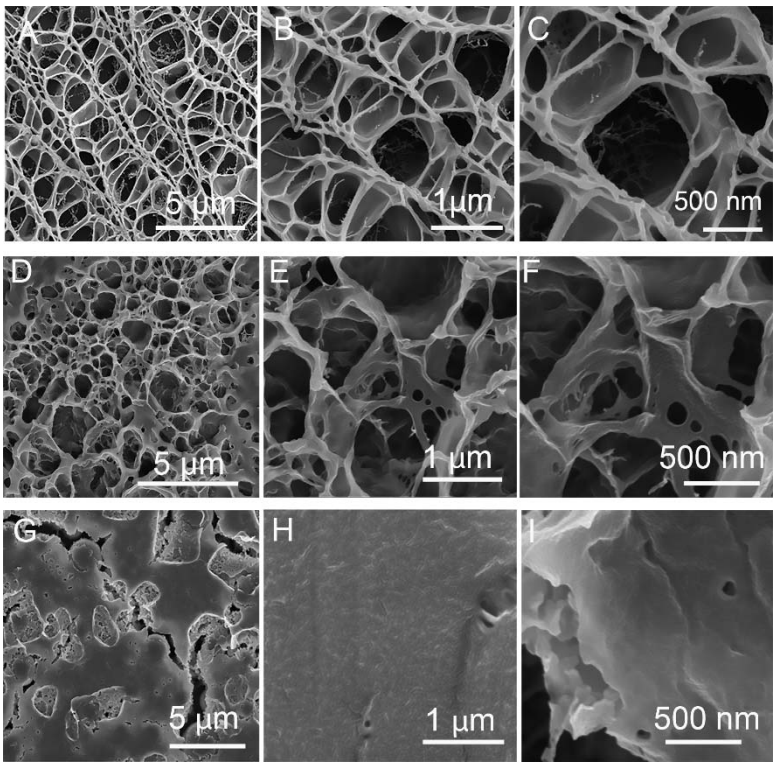

Figure 14. Scanning electron microscopy images of hydrogels and controls at 3 different magnifications. (A-C) DNA-crosslinked hydrogels. (D-E) PEG-crosslinked hydrogels. (G-I) Control non-gelling mixture of 4-Arm-PEG-NH_2 and amine-functionalized DNA (NH_2−GCTCCGTGCGAGGGTCGAGCCC−NH_2).

Nuclease-Dependent Degradation of Hydrogels

Initial studies of nuclease-dependent hydrogel degradation were performed with the use of the Benzonase®. Benzonase® is a non-sequence specific nuclease that degrades all forms of RNA and DNA by hydrolyzing internal phosphodiester bonds. This genetically engineered enzyme from *Serratia marcescens* is produced in *E. coli* and has no proteolytic activity.[66] Figure 15 shows phase contrast microscopy images of 0.3-µL-hydrogels when exposed to Benzonase® solution (5 U/mL) or the same volume and concentration of nuclease-free buffer over time. The control hydrogel crosslinked with PEG bisazide was observed to swell over the 45 minute time period after immersion in 50 µL of buffer but, as expected, no degradation was observed. Similarly, no

degradation was observed within 45 minutes upon addition of 50 µL of nuclease-free buffer to DNA-crosslinked PEG hydrogels. However, when the same gel was transferred to a well containing the 50 µL of Benzonase® solution, the gel degraded during the 45 minute time period as shown in Figure 4, indicating that the endonuclease cleaved the DNA, effectively disrupting hydrogel crosslinking. The degradation was not sudden, but rather occurred steadily over time.

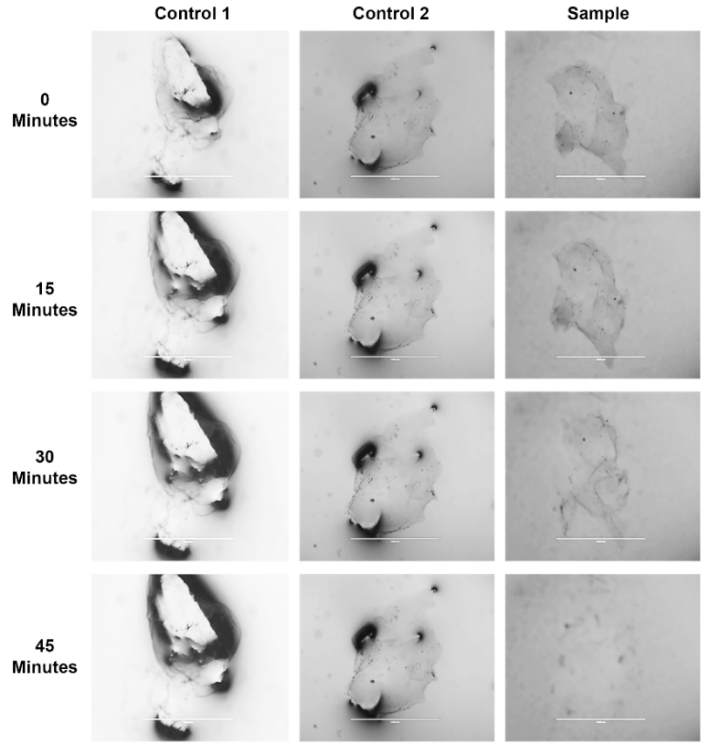

Figure 15. Nuclease-mediated degradation of DNA-crosslinked hydrogels. Phase contrast images were taken of individual hydrogels after exposure to 50 µL solutions of buffer or 5 U/mL benzonase® solution. Control 1: PEG-crosslinked hydrogel exposed to benzonase®. Control 2: DNA-crosslinked hydrogel exposed to PBS. Sample DNA-crosslinked hydrogel exposed to benzonase®. Scale bar represents 2000 µm.

Quantitative monitoring of hydrogel degradation was also performed in separate studies using a quartz crystal microbalance (QCM). QCM is commonly used to monitor gravimetric changes by tracking shifts in the resonant frequency of an oscillating quartz

crystal and relating it to mass changes through the Sauerbrey equation:

$$\Delta f = -\frac{2 f_0^{\,2} \Delta m}{A \rho_q^{\,1/2} \mu_q^{\,1/2}}$$

where ΔF is the change in frequency of the crystal (Hz), f_o is the resonance frequency characteristic of the crystal (Hz), Δm is the change in mass on the crystal (g), A is the surface area of the crystal (cm^2), ρ_Q is the density of quartz (2.648 g/cm^3) and μ_Q is the shear modulus of quartz (2.947 x 10^{11} $g/cm.s^2$).[67–70] The linear relationship between frequency and mass changes described by the Sauerbrey equation is most reliable when applied to homogeneous, rigid, non-viscoelastic films.[68,71] Nonetheless, decreases in mass due to hydrogel degradation will result in changes in crystal resonant frequency. [71,72]

For QCM studies, the more physiologically relevant DNase I nuclease was utilized at 291 U/mL, a concentration that is approximately 10-fold the reported serum DNase I activity in healthy individuals.[53] This nonspecific nuclease degrades both single and double-stranded DNA in a similar mechanism as Benzonase®. Figure 5 shows the values of ΔF over time with respect to initial frequency shifts ($\Delta F_t - \Delta F_o$). For the first 60 minutes, the initial frequency shift (ΔF_o) used for normalization was that of the system upon exposure to DNase-free buffer. For the second period (60 to 120 minutes), the initial frequency shift (ΔF_o) used was that of the system upon exposure to DNase solution. As shown in Figure 16, ΔF remained relatively constant when both the DNA-crosslinked hydrogel and the PEG-bisazide hydrogel were exposed to DNase-free buffer. An increase in ΔF was observed over time when the DNA-crosslinked hydrogel was exposed to the DNase I solution, indicating the degradation of the hydrogel leading to a decrease in hydrogel-induced dampening of the crystal resonance. The data indicate that degradation takes place at a high rate for a period of approximately 30 minutes, after which the rate of

degradation decreases. Alternatively, a decrease in ΔF was observed when the PEG-crosslinked hydrogel was exposed to the enzyme solution, especially over the first 30 minutes after exposure. The decrease in ΔF of the crystal with the PEG-crosslinked hydrogel is associated with the passive adsorption of the nuclease onto the surface of the quartz crystal and hydrogel, an event that was confirmed in separate experiments in the absence of hydrogels.

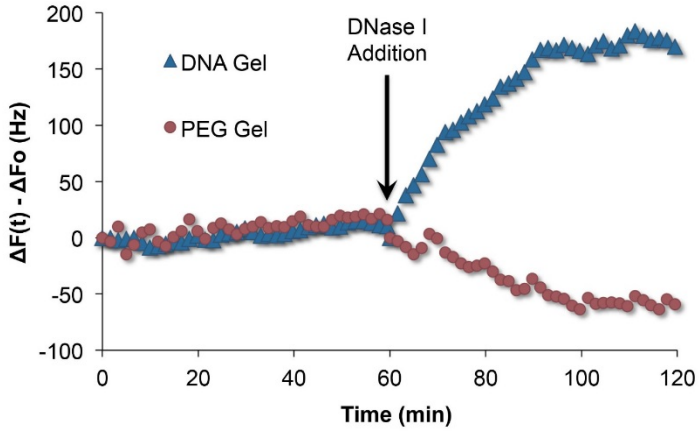

Figure 16. QCM studies of degradation. Kinetics of hydrogel biodegradation monitored by quartz crystal microbalance analysis. Data is presented as the relative change of crystal frequency compared to initial settings upon exposure of the respective hydrogel to buffer and DNase-solution.

Application of Nuclease-Induced Degradation in Controlled Delivery

Studies were performed to investigate the ability of the hydrogels to entrap model therapeutic cargo and deliver it upon nuclease-dependent degradation. These studies were carried out with DNase I at two concentrations: 1X = 29.1 U/mL and 10X = 291 U/mL which are equivalent to 1X and 10X the activity of DNase I in serum.[53] Figure 17 shows fluorescence images and mass of BSA-FITC released from these hydrogels over time upon exposure to DNase I solution.

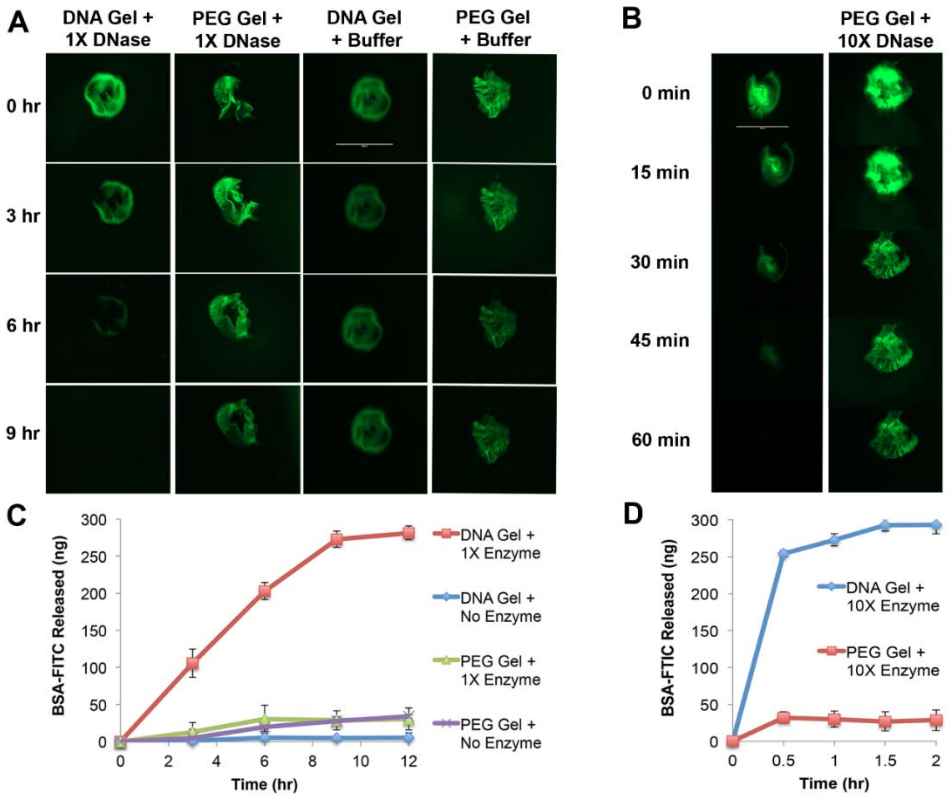

Figure 17. Nuclease-controlled release of BSA-FITC from hydrogels. (A and B) Fluorescence images of DNA- or PEG-crosslinked hydrogels loaded with BSA-FITC when exposed to DNase-free buffer, 1X DNase (29.1 U/mL), or 10X DNase (291 U/mL) as a function of time. Fluorescence intensity corresponds to level of BSA-FITC remaining within hydrogel. (C and D) Mass of BSA-FITC released to the surrounding from DNA- or PEG-crosslinked hydrogels exposed to DNase-free buffer, 1X DNase, or 10X DNase as a function of time. Data points represent average of three replicates and error bars represent their standard deviation. Note the different time scales for hydrogels exposed to buffer or 1X DNase (left) versus those exposed to 10X DNase (right).

As shown in the fluorescence images and accompanying plots in Figure 17, DNA-crosslinked hydrogels were able to deliver BSA-FITC over periods of 1 to 9 hours when exposed to DNase I at the 1X and 10X concentrations, respectively. Specifically, in the presence of 10X DNase a rapid release of BSA-FITC was observed within the first 30 minutes, after which the rate of release significantly decreased. When exposed to the 1X DNase concentration, BSA-FITC was released at an approximately constant rate over a period of 9 hours, after which little further release was observed. In contrast, neither DNA-crosslinked hydrogels in buffer or PEG-crosslinked hydrogels in either buffer or DNase solutions released the protein in significant amounts over the time periods studied.

The data presented confirms the feasibility of the preparation of DNA-enabled biodegradable hydrogels via copper-free click chemistry under physiological conditions. Biodegradable hydrogels have been used for a variety of applications including drug delivery and tissue engineering in the past as a result of their ability to incorporate proteins, cells, and drugs within their polymeric network.[73] With these capabilities, the hydrogels presented in this work have potential in various applications.

Conclusions

In this work, we present a method for the facile preparation of hydrogels from branched hydrophilic polymers that are crosslinked with single-stranded DNA. Specifically, copper-free click chemistry was utilized to prepare hydrogels from 4-Arm-PEG-DBCO and azide-functionalized DNA strands in saline solutions at room temperature. Degradation of these hydrogels was demonstrated using two non-sequence specific endonucleases, DNase I and Benzonase®. The ability of the hydrogels to release a model protein upon interaction with DNase I was also shown. This work demonstrates the potential of DNA crosslinked hydrogels as biodegradable systems that could have significant applications in biomedicine.

CHAPTER V

DESIGN AND PREPARATION OF ADENOSINE-RESPONSIVE HYDROGELS

Background

The inclusion of aptamers as functional building blocks can enable the preparation of "smart" materials that are called such due to their responsiveness to molecular or environmental stimuli. Hydrogels utilizing aptamers have not been extensively explored, but recent research has given promise that these hydrogels have potential for a variety of applications, from sensing to drug delivery.

The Tan group at the University of Florida has been prominent in the field of aptamer-based hydrogels and has designed a variety of systems that explore the potential of aptamers as material components in applications ranging from controlled release to colorimetric detection of molecules.[1,2] One of the earliest examples of aptamers in hydrogels reported by this group involves the adenosine aptamer and two partially complementary, acrydite-modified oligonucleotides, referred to as Strand A and Strand B.[3] These two oligonucleotides were separately polymerized with acrylamide, forming A and B polymeric precursors. When these precursor were mixed, they remained in solution. However, upon addition of a linker strand, composed of the adenosine-specific aptamer and an additional oligonucleotide extension that is partially complementary to both strands A and B, hybridization of the three strands caused crosslinking of the polymeric precursors and thereby formation of a hydrogel.[3] When adenosine was then added to the solution surrounding the gel, the aptamer-containing linker strand preferentially bound to adenosine and displaced its complementary oligonucleotide,

causing disruption of the crosslinking and dissolution of the hydrogel.[3] This is one method by which an aptamer strand can be incorporated into a polymeric hydrogel system as a functional material, and by which the molecular recognition of the target by the aptamer can trigger disassembly of the hydrogel. A system such as this could be used to release encapsulated cargo held within the intrinsically porous network of the hydrogel.[4]

An alternative approach that involves the use of aptamers as functional building blocks for hydrogel preparation is one that does not lead to disassembly of the hydrogel, but still achieves controlled release. This approach has the cargo to be delivered attached to an aptamer that is tethered to the hydrogel's polymeric network.[1] With this type of system, delivery of payloads can be achieved, but no interruption of crosslinking or disassembly of the hydrogel occurs. This case was illustrated by Liu and coworkers, who used gold nanoparticles decorated with the adenosine aptamer's complementary strand as the model cargo.[5] Upon recognition and binding of the aptamer strand to the target molecule adenosine, the gold nanoparticles would be released. This again shows the specificity of aptamers and the ability they have to play a role in systems designed for molecularly-controlled release.

Overall Design of Adenosine-Responsive Hydrogels

As with the other hydrogels presented in this thesis, 4-arm-PEG is used as the backbone of the hydrogel networks. The hydrogels described in this chapter are crosslinked by a DNA complex which includes an aptamer-containing linker DNA strand, and two partially complementary DNA strands, strands A and B. These three

hybridized strands together make up the hydrogel's crosslinking moiety and are termed the "aptamer complex" from here on. The design of these aptamer complexes is slightly modified from that reported by Yang *et al.*.[3] The adenosine aptamer was chosen for this work because it is a well-established and understood aptamer model.[6] This aptamer was chosen to design a model system that could be later expanded upon for systems responsive toward more physiologically relevant molecules.

The linker strand is composed of the adenosine aptamer (red and underlined in Figure 18) and an extending sequence (black in Figure 18). The aptamer portion of the linker strand is 27 nucleotides long, 20 of which are left unhybridized to enable interaction with the target adenosine molecules. Strand A (blue in Figure 18) is complementary to the extension portion of the linker strand and contains a fluorescent molecule, 6-fluorescein amidite (6-FAM), on the 5' end. Strand B (green in Figure 18) is complementary to five nucleotides of the linker's extension and seven of the nucleotides that are part of the aptamer sequence. Strand B is modified with a quenching molecule, BHQ1 (Black Hole Quencher®-1) on the 3' end (blue in Figure 18). The 3' end of strand A and the 5' end of strand B are both covalently linked to 4-arm-PEG molecules. Crosslinking of the hydrogel network is achieved by hybridization of strand A, strand B, and the linker strand.

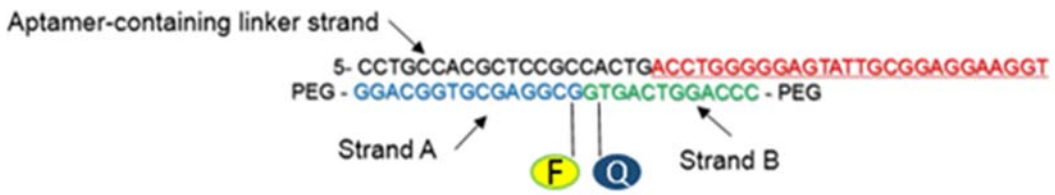

F = 6FAM Q = BHQ1

Figure 18. Sequences of the three strands used to form the hydrogel's crosslinking aptamer complex.

Figure 19A illustrates how the hybridized DNA aptamer complex serves as the crosslinking moiety when adenosine is not present in the environment. When adenosine is present in the environment, the aptamer portion of the linker strand will preferentially bind to adenosine and displace strand B (Figure 19B). When strand B is displaced, the crosslinking aptamer complex is disrupted, therefore causing degradation of the hydrogel.

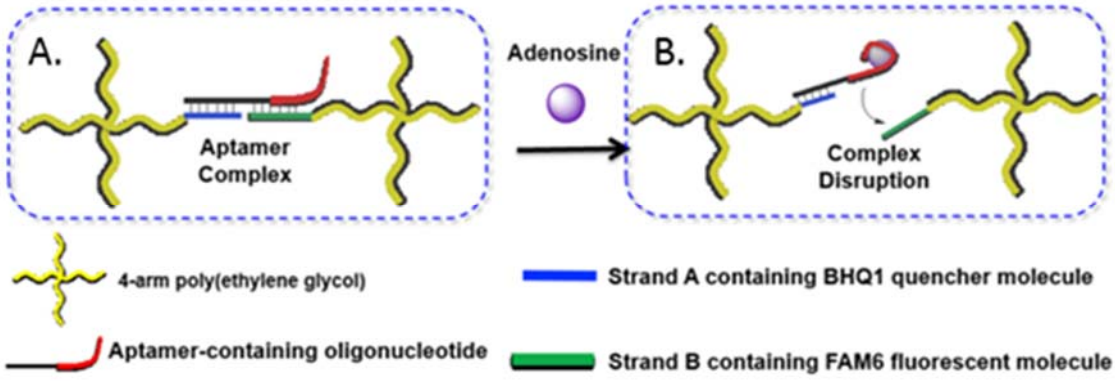

Figure 19. System 2 overview. **(A)** Design of the hydrogel network where strands A and B are hybridized to the linker strand forming the crosslinking aptamer complex. **(B)** Addition of adenosine causes disruption of the crosslinking aptamer complex upon preferential binding of the aptamer to its target.

There are two approaches presented in this chapter for the formation of these molecularly responsive, aptamer complex crosslinked hydrogels: (1) click chemistry-

driven assembly, and (2) hybridization-driven assembly. These methods are described below.

Click-driven hydrogel formation

With click-driven hydrogels, it is the interaction between azide-functionalized aptamer complexes and highly strained, alkyne containing DBCO molecules on the 4-arm-PEG-DBCO precursor that causes formation of the hydrogel. In this method, hybridization of azide-terminated aptamer complexes occurs prior to reaction of these complexes with 4-arm-PEG-DBCO, as shown in Figure 20. The hybridization process is done by heating equimolar ratios of strand A, strand B, and the linker strand to 95 ºC to dehybridize any secondary structures the DNA may have formed, and letting the solution cool to room temperature, allowing for the strands to form the aptamer complex that will serve as the crosslinking moiety. Successful formation of hydrogels using this method of gelation is demonstrated in this work in Section 5.5.

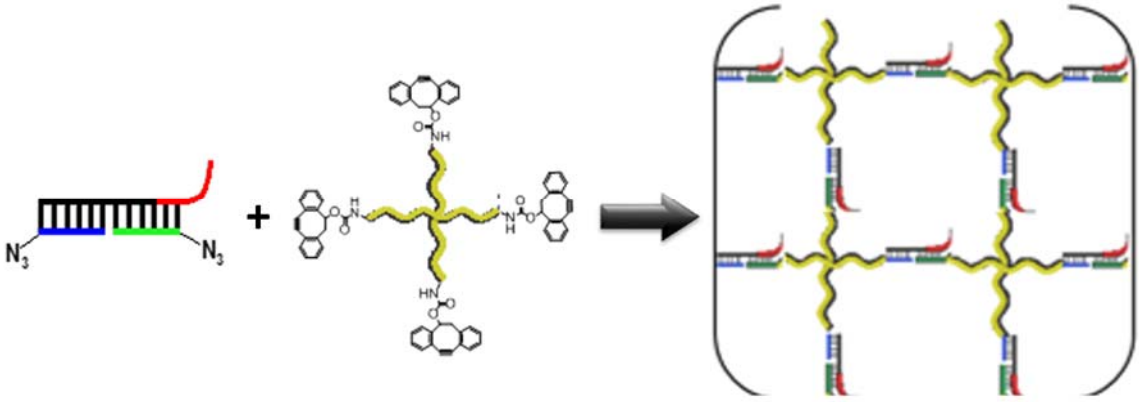

Figure 20. Formation of a hydrogel using the click-driven method.

Hybridization-driven hydrogel formation

With hybridization-driven formation, 4-arm-PEG molecules are first covalently functionalized with the respective DNA oligonucleotides (either Strand A or Strand B) on all four ends (Figure 21). When the two solutions of oligonucleotide-functionalized PEG are combined, a gel is not expected to form. However, upon addition of the linker strand and heating to 95 ºC, the linker strand drives the formation of the hydrogel by hybridizing to the complementary DNA arms on PEG. A portion of the aptamer sequence on the linker strand is unhybridized and therefore able to interact with adenosine when present in the environment. In this case, it is hybridization causing the assembly of the hydrogel, as opposed to a covalent chemical reaction, as was described with the click-driven hydrogel formation process.

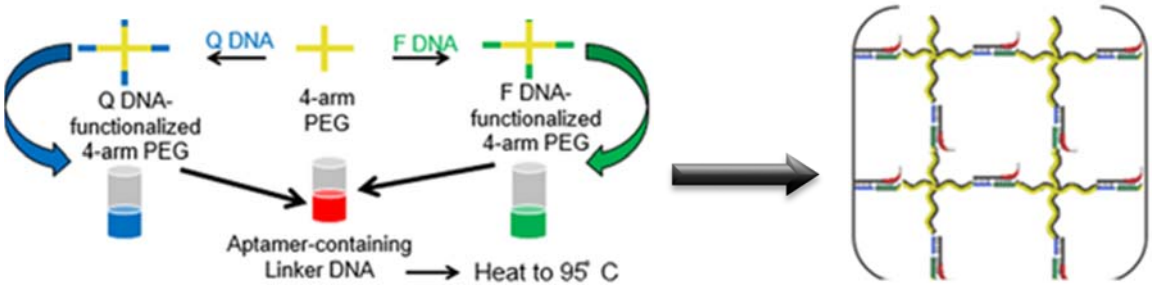

Figure 21. Formation of hydrogel through the hybridization-driven method.

5.3 Confirmation of Complex Formation

Before the use of the oligonucleotides in the formation of hydrogels by either click chemistry- or hybridization-driven assembly, the complexation, stability, and target response of these hybridized DNA complexes had to be demonstrated. To carry out these studies, the oligonucleotides listed in Table 1 were utilized. These oligonucleotides were

obtained from Integrated DNA Technologies.

Table 1. Oligonucleotide Sequences Used for Formation of Aptamer Complexes

Strand Name	Strand Sequence	# of Nucleotides
Strand A	5' GCGGAGCGTGGCAGG-***6FAM*** 3'	15
Strand B	5' ***BHQ1***-CCCAGGTCAGTG 3'	10
Linker	5' CCTGCCACGCTCCGCTCACTGACCTGG GGGAGTATTGCGGAGGAAGGT 3'	48

Abbreviations: 6FAM = 6-fluorescein amidite, BHQ1 = Black Hole Quencher®-1

For these studies, DNA was dissolved in Tris buffer pH 9.5 (30 mM NaCl, 0.5 mM $MgCl_2$). The sample complex contained an equimolar ratio of all three strands, which were all prepared at a concentration of 10 nM. The sample was heated to 95 ºC for five minutes and then cooled to room temperature.

In order to verify hybridization of the DNA complex, agarose gel electrophoresis was used. Agarose powder was obtained from Gold Biotechnology, Olivette, MO. A 3% percent agarose gel was prepared and run at 250 V for 30 minutes after loading samples (Figure 22). In order to image the sample bands, the gel was stained with 0.625 mg/ml ethidium bromide (EtBr) solution (Thermo Scientific, Waltham, MA), which is a dye that binds specifically to DNA by intercalating between bases. Using a Red™ Personal Imaging System, an image of the gel and DNA bands was acquired. Lane 1 was loaded with the O'RangeRuler 10 bp DNA ladder from Thermo Scientific. Lanes 2 and 3 had 0.05 pmol of strands A and B, respectively. Lane 4 contained 0.05 pmol of each strands A, B, and linker together. Based on the migration of the band in lane 4 which contained all three components of the DNA complex and comparison to the corresponding ladder in

lane 1, it can be seen that the complex did in fact form. No separate bands were present for the A and B strands in lane 4, most likely due to the fact that the amount of these strands left unhybridized was below the detection limit with EtBr, and therefore did not show fluorescence under UV light.

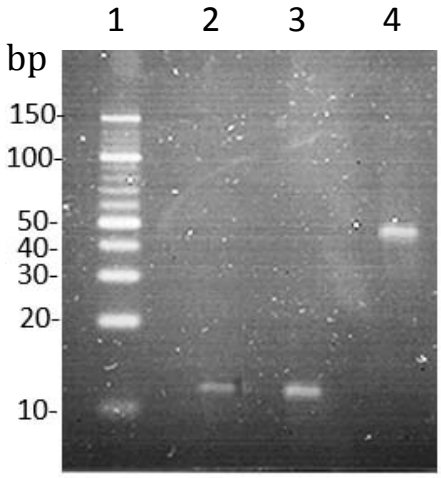

Figure 22. Agarose of complex. 3% Agarose gel stained with EtBr to confirm formation of DNA complex. Lane 1: 10 bp ladder, lane 2: strand A, lane 3: strand B, lane 4: strands A, B, and linker.

5.3 Thermal Studies of DNA Complex

In order to verify that the DNA complex is stable at physiological temperature, thermal studies were performed. Complex dissociation was monitored via fluorescence spectroscopy using a Biotek Synergy H4 multi-mode plate reader with a Take3 micro-volume plate. For these studies, DNA was dissolved in Tris buffer pH 9.5 (30 mM NaCl, 0.5 mM $MgCl_2$). The sample complex contained an equimolar ratio of all three strands, which were all prepared at a concentration of 10 nM. As the temperature increases, the three-part complex is expected to dissociate resulting in an increase in fluorescence intensity. The fluorescence of the samples was monitored from 28 to 64 ºC. The

fluorescence data of the complex was normalized to that of the control (mixture of FAM6-labeled strand A and BHQ1-labeled strand B in the absence of the linker strand) to account for instrumental drift.

After plotting fluorescence vs. temperature, a sigmoidal curve is seen (Figure 23). The halfway point of the curve corresponds to the melting temperature of the complex, the temperature at which half of the DNA hybridized and half is single-stranded (Figure 6). It was determined that the complex is stable at physiological temperature of 37 ºC and has a melting temperature of ca. 51 ºC. The expected melting temperatures provided by Integrated DNA Technologies OligoAnalyzer are 61.9 ºC and 44 ºC for strand A and its perfect complement and for strand B and its perfect complement, respectively (using the following ion concentrations: 50 mM Na^+, 0.5 mM Mg^{2+}). The data obtained matches the expected behavior of the aptamer complex. Significant complex disruption begins at temperatures over 40 ºC, demonstrating the stability of this complex at room and physiological temperature.

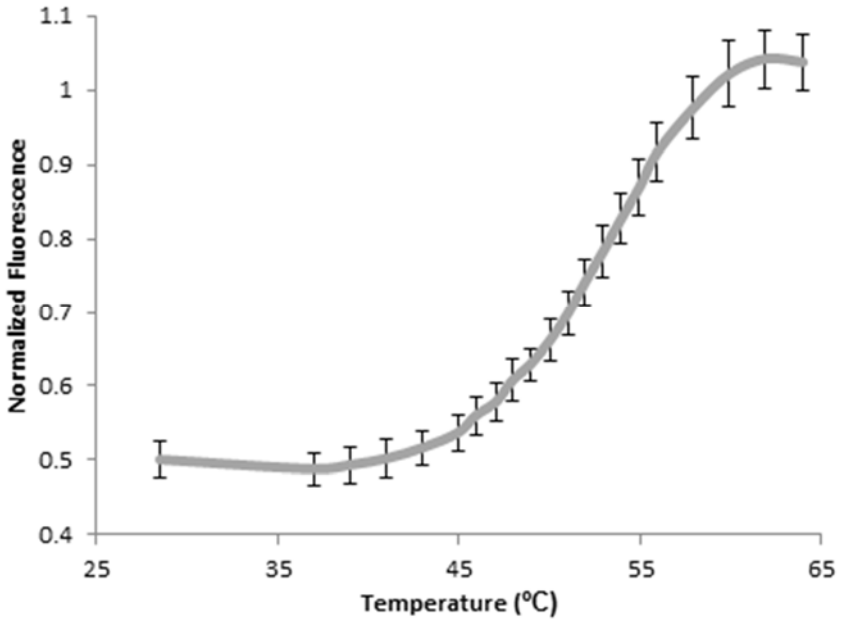

Figure 23. Determination of the melting temperature of the DNA complex. Error bars represent the standard deviations between replicates (n =5).

5.4 Adenosine-triggered Dissociation of Complex

Before forming a hydrogel containing this complex, the response of the complex in buffer solution to the presence of adenosine was monitored using fluorescence spectroscopy (Figure 24). In buffer solution, DNA is complexed as shown on the left of Figure 24. In this complexed state, the close proximity of the fluorophore and quencher molecules enables Forster resonance energy transfer (FRET) between the fluorophore and the quencher, leading to fluorescence quenching. Upon addition of adenosine, the aptamer preferentially binds to adenosine, effectively displacing strand B. Complex dissociation prevents FRET from occurring, due to increased distance between the FAM6 (F) molecule and the BHQ1 (Q) molecule. Therefore, an increase in fluorescence is detected upon addition of adenosine and complex disruption.

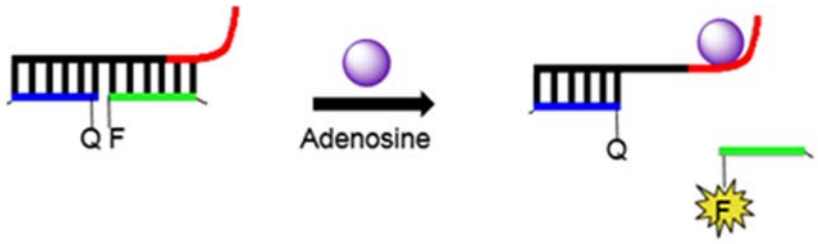

Figure 24. FRET studies. Illustration of how fluorescence was used to monitor dissociation of the DNA complex when the target adenosine is introduced.

DNA was again dissolved in Tris buffer pH 9.5 (30 mM NaCl, 0.5 mM $MgCl_2$). The sample complex contained a 1:1:1 ratio of strand A: strand B: linker strand at a concentration of 10 nM. As a control, a solution of strand A and strand B at the same concentration as the sample was used. The sample and controls were exposed to adenosine solutions or to the same volume of Tris buffer and the fluorescence was monitored at room temperature. The complex showed an increase in fluorescence intensity upon addition of 3 mM and 6 mM solutions of adenosine in Tris buffer (Figure 25, left), indicating that the complex had been disrupted. Dilution of the aptamer complex with the same volume of buffer had little effect on the sample fluorescence. Also, neither adenosine nor buffer solutions had a significant effect on the fluorescence of the controls (Figure 25, right). These data demonstrate that the complex dissociates when adenosine is present, likely due to the aptamer portion of the linker strand having higher affinity toward the adenosine molecules than to the partial complementary strand B.

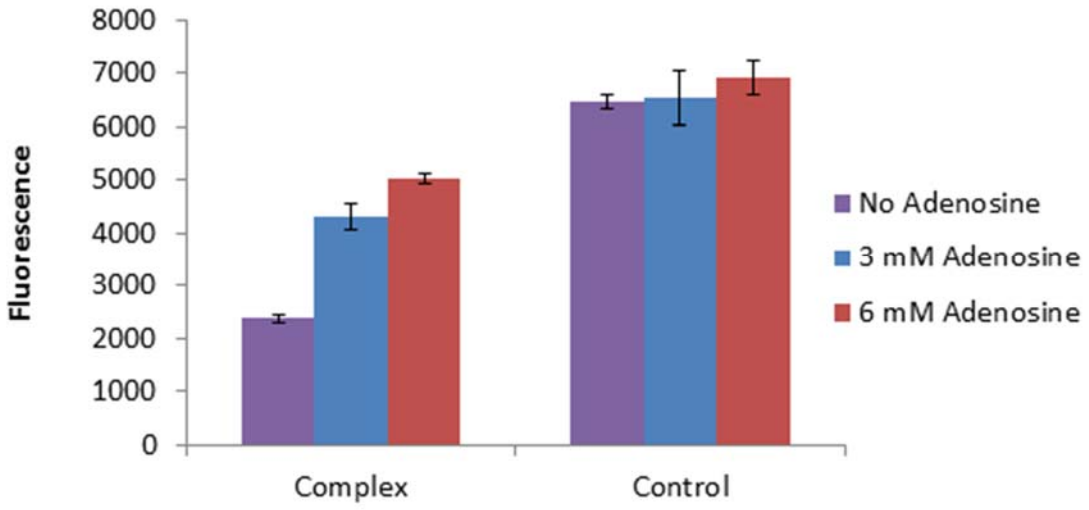

Figure 25. Adenosine-induced dehybridization of aptamer complex. Error bars represent the standard deviation between replicates (n = 5).

Successful Click Chemistry-Driven Hydrogel Formation

Table 2 summarizes the sequences of the oligonucleotides used in the preparation of the click chemistry-driven hydrogels. These oligonucleotides were obtained from Integrated DNA Technologies functionalized with azide groups on the 3' end of strand A and the 5' end of strand B. The solutions of each strand, A, B, and linker were prepared in Tris buffer pH 9.5 (30 mM NaCl, 0.5 mM $MgCl_2$). Approximately 3.5 nmol of each of the three strands were mixed together to a total volume of 0.15 µL. This solution was then heated to 95 ºC on an Eppendorf thermomixer for two minutes and cooled to room temperature in order to allow hybridization of the three strands to occur.

A volume of 0.15 µL of 200 mg/mL 4-arm-PEG-DBCO was then mixed with the 0.15 µL of the hybridized DNA solution, giving an overall polymer weight percent of 20 % w/v. After a fifteen minute gelation period, the hydrogels were observed on a microscope to ensure that the hydrogels had formed (Figure 26A).

Table 2. Oligonucleotide Sequences Used for Click-Driven Hydrogel Formation

Strand Name	Strand Sequence
Strand A	5' GCGGAGCGTGGCAGG- **N_3** 3'
Strand B	5' **N_3**-CCCAGGTCAGTG -**N_3** 3'
Linker	5' CCTGCCACGCTCCGCTCACTGACCT GGGGGAGTA TTGCGGAGGAAGGT 3'

Hydrogel Response to Adenosine

A 0.30 µL sample hydrogel (Figure 26A) was first exposed to 5 µL of 2 mM Tris buffer pH 7.5 to investigate whether a hydrogel had been formed. As expected, after 15 minutes the hydrogel still remained intact (Figure 26B). The surrounding buffer solution was then removed and 5 µL of 6 mM adenosine solution was then added to the same hydrogel. Two minutes after addition of this solution, the hydrogel was already beginning to degrade (Figure 26C). After five minutes, full dissolution of the hydrogel was observed (Figure 26D). Buffer solution was first added to ensure that the disassembly of the hydrogel was due to the interaction of the aptamer with adenosine and not due to dissolution of the un-crosslinked hydrogel precursors. As shown, the hydrogel did not degrade in the presence of buffer solution, indicating that it was in fact the presence of adenosine that caused its degradation. Further studies will need to be performed in order to gather a better understanding of the properties of these hydrogels and their potential as materials for drug delivery, wound healing, or biosensing applications.

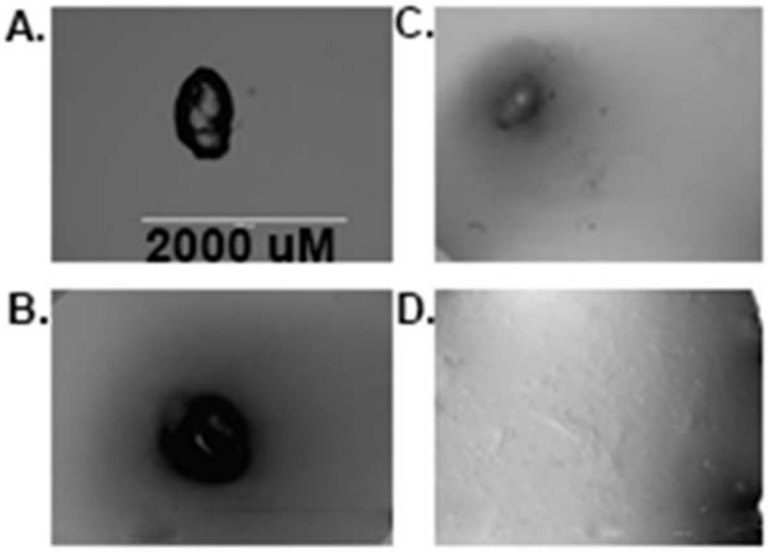

Figure 26. Click chemistry aptamer complex hydrogel. **(A)** DNA-crosslinked hydrogel made by click chemistry-driven formation method. **(B)** Five minutes after addition of 5 µL of buffer solution. **(C)** Two minutes after addition of 5 µL of 6 mM adenosine solution. **(D)** Five minutes after addition of adenosine.

Preparation of 4-arm-PEG-oligonucleotide Conjugates for Hybridization-Induced Hydrogel Assembly

To prepare the PEG-DNA precursors, N-hydroxysuccinimide (NHS) esters of 4-arm-PEG (Laysan Bio, Arab, AL) were reacted with primary amines present on one end of each of the DNA strands, resulting in stable amide bonds. Oligonucleotides were obtained from Eurofins. Table 3 summarizes the sequences and modifications of these oligonucleotides.

Table 3. Oligonucleotide Sequences for Hybridization-Induced Hydrogel Assembly

Strand Name	Strand Sequence
Strand A	5’GCGGAGCGTGGCAGG[AmC7~Q]3’
Strand B	5’[AminoC6]CCCAGGTCAGTG 3’
Linker	5’CCTGCCACGCTCCGCTCACTGACCTGG GGGAGTATTGCGGAGGAAGGT 3’

Abbreviation: AmC7 =3' amino modifier. AminoC6 =5' amino modifier

The NHS ester terminated PEG used for these reactions was the 4-arm-PEG succinimidyl glutarate ester (4-arm-PEG SG, MW 10,000) (Figure 27). 4-arm-PEG SG was prepared at a concentration of 0.5 μM. The reaction of 4-arm-PEG SG and DNA oligonucleotides (either Strand A or Strand B) was done in 2 mM Tris buffer at a molar ratio of 8:1 DNA:4-arm-PEG SG, giving a two-fold molar excess of DNA. The reaction was performed at room temperature and reacted overnight, leading to the attachment of DNA to the terminal ends of the PEG chains via amide bonds.

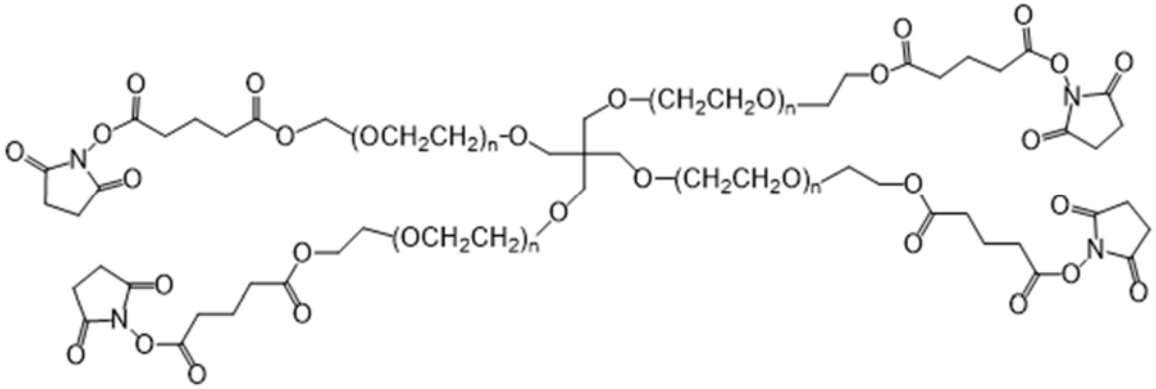

Figure 27. Structure of 4-arm-PEG SG.

HPLC Purification of 4-Arm-PEG-DNA Conjugates

In order to separate the components of the reaction and purify the product (4-arm-PEG-DNA conjugtates), high-performance liquid chromatography (HPLC) was used. For the hydrogel to form as expected, it is necessary to separate out the PEG molecules that are fully functionalized on all four arms from those that are not, as well as to separate excess DNA.

For HPLC separation, a Varian ProStar 320 HPLC with a Waters C18 reverse

phase column (4.6 mm x 150 mm) was used. The solvents used for the mobile phase were water and acetonitrile. Starting at 100% water, the percent acetonitrile increased at a rate of 1.67% per minute for the first three minutes followed by a rate of increase of 13.6% acetonitrile per minute until reaching 100% acetonitrile. The percent acetonitrile was then decreased at a rate of 20% per minute until reaching 100% water. The volume of sample injected was 20 μL. The flow rate remained constant at 1 mL/minute. Absorbance was measured at the wavelength of 254 nm allowing for the detection of DNA, which absorbs strongly at that wavelength.

One of the byproducts of the reaction between 4-arm-PEG SG and amine-modified DNA is N-hydroxysuccinimide (NHS), which is small and very polar and therefore should elute the fastest. Because DNA is so polar, it would be expected that the excess, unbound DNA would elute faster than the 4-arm-PEG-oligo conjugates. As the 4-arm-PEG increases in the number of functionalized arms, from one arm containing DNA, to being fully conjugated on all fur arms, the polarity of the molecule increases. This would mean that fully functionalized PEG would elute faster than PEG with only one arm containing DNA. Without DNA on PEG, an absorbance signal would not be detected, unless NHS did not hydrolyze off during the twenty-four hour reaction period. The retention time for amine-functionalized DNA by itself is around 1.1 minutes (Figure 28A) and a signal with this retention time is also seen in Figure 28B, which is the chromatogram of the reaction mixture. Because the reaction was done at a high molar excess of DNA, it would be expected that there would be a strong signal for unbound DNA. The fully functionalized 4-arm-PEG-DNA product is thought to be eluting at a retention time of 1.5 minutes, while the subsequent signals are likely due to 4-arm-PEG

decreasing in the number of functionalized arms. In order to test this, NMR was run of the collected HPLC fractions.

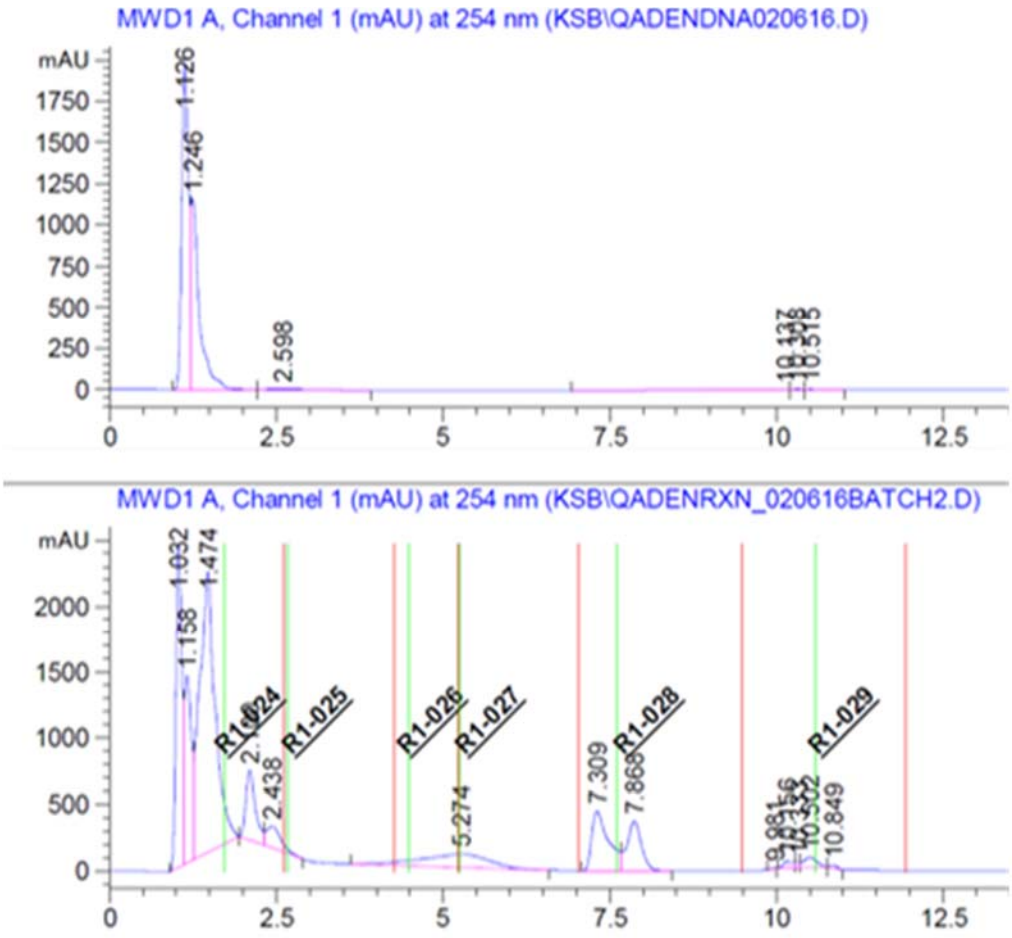

Figure 28. HPLC chromatograms. **(A)** amine-functionalized DNA and **(B)** reaction mixture with wavelength measured at 254 nm.

Two NMR spectra were gathered: one of the first three fractions collected from HPLC, and one of the remaining three fractions. ^{1}H NMR done in deuterated water (D_2O). In both spectra, PEG is present, which shows a signal at 3.6 ppm (Figures 29A and 29B).

A.

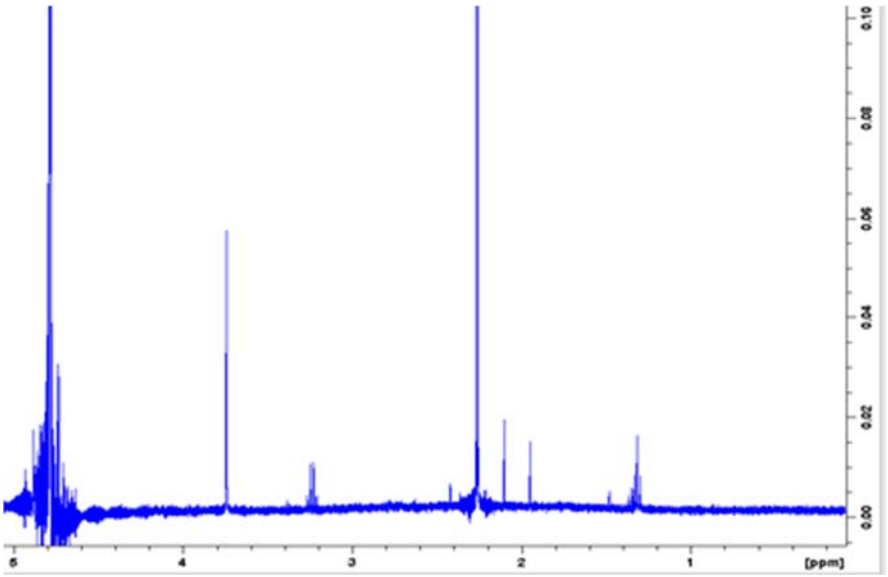

B.

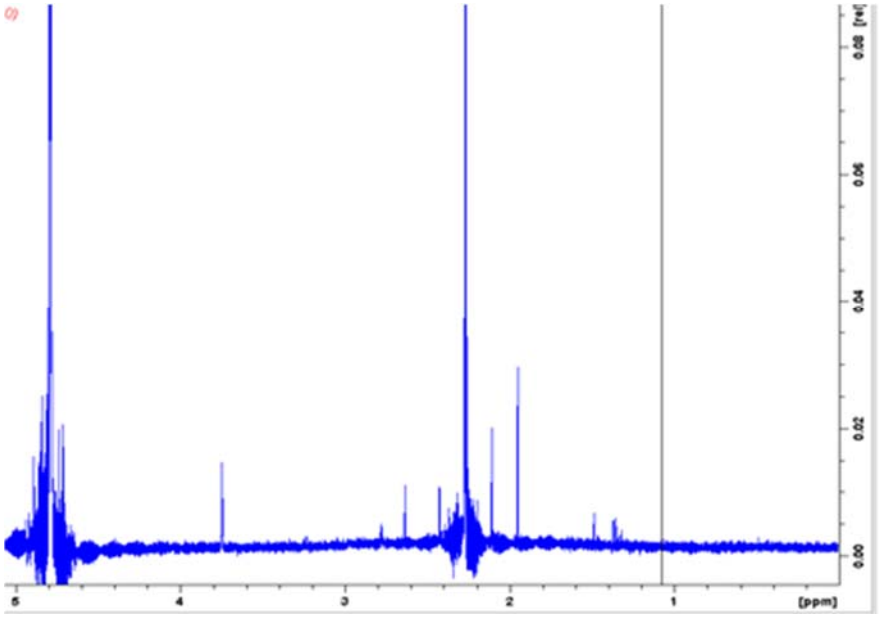

Figure 29. NMR spectrum of HPLC fractions. **(A)** ^{1}H NMR spectrum of the first 3 fractions collected from HPLC purification. **(B)** NMR of last 3 fractions.

The signal at 2.2 ppm is from acetone, which is due to the NMR tubes not being completely dry after cleaning them with acetone, while the signal at 4.8 ppm is from residual water in D_2O. It should be noted that the fractions were combined and concentrated in order to obtain high enough sample concentrations to enable detection of DNA and PEG.

Because PEG is not nearly as polar as DNA, it would not be expected to elute so quickly off the column where there is such a high concentration of water unless its polarity was increased drastically by the presence of the four conjugated DNA strands. Since a signal for PEG was seen in both NMR spectra, it supports the above theory that the fully functionalized conjugate elutes early in the run, while the peaks at later retention time could be due to 4-arm-PEG functionalized with a decreasing number of DNA strands.

Future work in this project will be to optimize the conjugate purification protocol in order to obtain sufficient pure 4-arm-PEG-DNA conjugates that can be used for hybridization-induced hydrogel assembly. With the current method, hydrogel assembly by hybridization was not successfully demonstrated. In addition to HPLC, gel electrophoresis could be explored as an alternative conjugate purification method.

Conclusions

Hydrogels were successfully formed using click chemistry with a three stranded aptamer complex as the crosslinker. Degradation of the hydrogel upon addition of adenosine solution indicates that the aptamer portion of the linker strand does preferentially bind to its target, displacing its complementary strand B and thereby

disrupting the hydrogel crosslinks. Further studies will need to be done in order to gain an understanding about the mechanical properties of these hydrogels. The HPLC purified product of the 4-arm-PEG-oligonucleotide conjugate will also be used to form hybridization-driven hydrogels.

CHAPTER VI

CONCLUSIONS

Conclusions

This work has demonstrated the preparation of PEG hydrogels with DNA serving as the crosslinker. Copper-free click chemistry was successful in making hydrogels in an aqueous environment. It was shown that hydrogels with ssDNA as the crosslinking molecule could be degraded by endonucleases in a controllable fashion dependent upon enzyme concentration. This work also illustrated the ability of these hydrogels to encapsulate a target protein and release it upon degradation triggered by cleavage of DNA crosslinking by the endonucleases.

It was also shown that copper-free click chemistry could be used in making hydrogels that had a dsDNA complex as the crosslinking moiety. With the inclusion of the adenosine aptamer sequence, the hydrogel showed responsiveness to the presence of adenosine. These hydrogels will need to be explored further in order to gather a better understanding of the properties and applications of these types of gels.

The adenosine-responsive hydrogels demonstrated the applicability of aptamers as biomaterial components. Using the system shown here as a model, other aptamer strands could be incorporated to make hydrogels that respond to molecules that are more physiologically relevant. By taking advantage of molecules that are characteristically present in a particular environment, hydrogels can be designed with high specificity for a wide variety of applications.

REFERENCES

(1) Samal, S. K.; Dash, M.; Dubruel, P.; Vlierberghe, S. Van. *Smart polymer hydrogels: properties, synthesis and applications*; Woodhead Publishing Limited, 2014.

(2) Soppimath, K. S.; Aminabhavi, T. M.; Dave, A. M.; Kumbar, S. G.; Rudzinski, W. E. *Drug Dev. Ind. Pharm.* **2002**, *28*, 957–974.

(3) Buwalda, S. J.; Boere, K. W. M.; Dijkstra, P. J.; Feijen, J.; Vermonden, T.; Hennink, W. E. *Journal of Controlled Release*. 2014, pp 254–273.

(4) Lin, D. C.; Yurke, B.; Langrana, N. A. *J. Biomech. Eng.* **2004**, *126*, 104–110.

(5) Xiong, X.; Wu, C.; Zhou, C.; Zhu, G.; Chen, Z.; Tan, W. *Macromol. Rapid Commun.* **2013**, *34* (16), 1271–1283.

(6) Lin, C. C.; Anseth, K. S. *Pharm. Res.* **2009**, *26* (3), 631–643.

(7) Knop, K.; Hoogenboom, R.; Fischer, D.; Schubert, U. S. **2010**, 6288–6308.

(8) Kolate, A.; Baradia, D.; Patil, S.; Vhora, I.; Kore, G.; Misra, A. *J. Control. Release* **2014**, *192*, 67–81.

(9) Kolate, A.; Baradia, D.; Patil, S.; Vhora, I.; Kore, G.; Misra, A. *J. Control. Release* **2014**, *192*, 67–81.

(10) Alconcel, S. N. S.; Baas, A. S.; Maynard, H. D. *Polym. Chem.* **2011**, *2* (7), 1442.

(11) Rani, K.; Paliwal, S. **2014**, *2*, 328–331.

(12) Lu, Y.; Liu, J. *Current Opinion in Biotechnology*. 2006, pp 580–588.

(13) Ellington, A. D. *Curr. Biol.* **1994**, *4* (5), 427–429.

(14) Ellington, a D.; Szostak, J. W. *Nature* **1990**, *346* (6287), 818–822.

(15) Lipman, N. S.; Jackson, L. R.; Weis-Garcia, F.; Trudel, L. J. *ILAR J.* **2005**, *46* (3), 258–268.

(16) Burns, R. *Methods Mol. Biol.* **2005**, *295*, 41–54.

(17) Nelson, P. N.; Reynolds, G. M.; Waldron, E. E.; Ward, E.; Giannopoulos, K.; Murray, P. G. *Mol. Pathol.* **2000**, *53* (3), 111–117.

(18) Weiner, L. M.; Surana, R.; Wang, S. *Nat. Rev. Immunol.* **2010**, *10* (5), 317–327.

(19) Nimjee, S. M.; Rusconi, C. P.; Sullenger, B. a. *Annu. Rev. Med.* **2005**, *56* (FEBRUARY), 555–583.

(20) Song, K. M.; Lee, S.; Ban, C. *Sensors* **2012**, *12* (1), 612–631.

(21) Lakhin, a V; Tarantul, V. Z.; Gening, L. V. **2013**, *5* (19), 34–43.

(22) Mastronardi, E.; Foster, A.; Zhang, X.; DeRosa, M. C. *Sensors (Basel).* **2014**, *14*, 3156–3171.

(23) Stoltenburg, R.; Reinemann, C.; Strehlitz, B. **2007**, *24*, 381–403.

(24) Qiu, Y.; Park, K. *Adv. Drug Deliv. Rev.* **2012**, *64*, 49–60.

(25) Thomas, J. B.; Tingsanchali, J. H.; Rosales, A. M.; Creecy, C. M.; McGinity, J. W.; Peppas, N. a. *Polymer (Guildf).* **2007**, *48* (17), 5042–5048.

(26) Koetting, M. C.; Peppas, N. a. *Int. J. Pharm.* **2014**, *471* (1-2), 83–91.

(27) Betancourt, T.; Pardo, J.; Soo, K.; Peppas, N. a. *J. Biomed. Mater. Res. - Part A* **2010**, *93* (1), 175–188.

(28) Klouda, L.; Mikos, A. G. *Eur. J. Pharm. Biopharm.* **2008**, *68*, 34–45.

(29) Zhao, Y. L.; Fraser Stoddart, J. *Langmuir* **2009**, *25* (15), 8442–8446.

(30) Huebsch, N.; Kearney, C. J.; Zhao, X.; Kim, J.; Cezar, C. a; Suo, Z.; Mooney, D. J. *Proc. Natl. Acad. Sci. U. S. A.* **2014**, *111* (27), 9762–9767.

(31) Yang, H.; Liu, H.; Kang, H.; Tan, W. *J. Am. Chem. Soc.* **2008**, *130*, 6320–6321.

(32) Wei, B.; Cheng, I.; Luo, K. Q.; Mi, Y. *Angew. Chemie - Int. Ed.* **2008**, *47*, 331–333.

(33) Nagahara, S.; Matsuda, T. *Polym. Gels Networks* **1996**, *4* (2), 111–127.

(34) Kang, H.; Liu, H.; Zhang, X.; Yan, J.; Zhu, Z.; Peng, L.; Yang, H.; Kim, Y.; Tan, W. *Langmuir* **2011**, *27*, 399–408.

(35) Xing, Y.; Cheng, E.; Yang, Y.; Chen, P.; Zhang, T.; Sun, Y.; Yang, Z.; Liu, D. *Adv. Mater.* **2011**, *23* (9), 1117–1121.

(36) Kolb, H. C.; Finn, M. G.; Sharpless, K. B. *Angewandte Chemie - International Edition*. 2001, 2004–2021.

(37) Tornøe, C. W.; Christensen, C.; Meldal, M. *J. Org. Chem.* **2002**, *67* (9), 3057–3064.

(38) Rostovtsev, V. V.; Green, L. G.; Fokin, V. V.; Sharpless, K. B. *Angew. Chemie - Int. Ed.* **2002**, *41* (14), 2596–2599.

(39) Chang, P. V; Prescher, J. a; Sletten, E. M.; Baskin, J. M.; Miller, I. a; Agard, N. J.; Lo, A.; Bertozzi, C. R. *Proc. Natl. Acad. Sci. U. S. A.* **2010**, *107* (5), 1821–1826.

(40) Baskin, J. M.; Prescher, J. a; Laughlin, S. T.; Agard, N. J.; Chang, P. V; Miller, I. a; Lo, A.; Codelli, J. a; Bertozzi, C. R. *Proc. Natl. Acad. Sci. U. S. A.* **2007**, *104* (11), 16793–16797.

(41) Jewett, J. C.; Bertozzi, C. R. *Chem. Soc. Rev.* **2010**, *39* (4), 1272–1279.

(42) Marks, I.; Kang, J.; Jones, B.; Landmark, K.; Cleland, A.; Taton, T. **2013**, *22* (7), 1259–1263.

(43) Kettenbach, K.; Ross, T. L. *Med. Chem. Commun.* **2016**, 16–19.

(44) Almutairi, A.; Rossin, R.; Shokeen, M.; Hagooly, A.; Ananth, A.; Capoccia, B.; Guillaudeu, S.; Abendschein, D.; Anderson, C. J.; Welch, M. J.; Fréchet, J. M. *Proc Natl Acad Sci U S A* **2009**, *106* (3), 685–690.

(45) Yamagishi, K.; Sawaki, K.; Murata, A.; Takeoka, S. *Chem. Commun.* **2015**, *51* (37), 7879–7882.

(46) Yamagishi, K.; Sawaki, K.; Murata, A.; Takeoka, S. *Chem. Commun.* **2015**, *51* (37), 7879–7882.

(47) Ledin, P. a.; Kolishetti, N.; Boons, G. J. *Macromolecules* **2013**, *46*, 7759–7768.

(48) Ning, X.; Guo, J.; Wolfert, M. A.; Boons, G. J. *Angew. Chemie - Int. Ed.* **2008**, *47* (12), 2253–2255.

(49) Zheng, J.; Liu, K.; Reneker, D. H.; Becker, M. L. *J. Am. Chem. Soc.* **2012**, *134* (41), 17274–17277.

(50) Li, S.; Chen, N.; Zhang, Z.; Wang, Y. *Biomaterials* **2013**, *34* (2), 460–469.

(51) Tian, Y. Z.; Li, Y. L.; Wang, Z. F.; Jiang, Y. *J. Mater. Chem. B* **2014**, *2* (12), 1667–1672.

(52) Kishi, K.; Yasuda, T.; Takeshita, H. *Leg. Med.* **2001**, *3* (2), 69–83.

(53) Yasuda, T.; Iida, R.; Kawai, Y.; Nakajima, T.; Kominato, Y.; Fujihara, J.; Takeshita, H. *Leg. Med.* **2009**, *11* (SUPPL. 1), S213–S215.

(54) Kominato, Y.; Iida, R.; Nakajima, T.; Tajima, Y.; Takagi, R.; Makita, C.; Kishi, K.; Ueki, M.; Kawai, Y.; Yasuda, T. *Biochim. Biophys. Acta* **2007**, *1770* (11), 1567–1575.

(55) Yasuda, T.; Kawai, Y.; Ueki, M.; Kishi, K. *Leg. Med.* **2005**, *7* (4), 274–277.

(56) Spandidos, D. A.; Ramandanis, G.; Garas, J.; Kottaridis, S. D. *Eur. J. Cancer* **1980**, *16* (12), 1615–1619.

(57) Al-Attar, a; Gossage, L.; Fareed, K. R.; Shehata, M.; Mohammed, M.; Zaitoun, a M.; Soomro, I.; Lobo, D. N.; Abbotts, R.; Chan, S.; Madhusudan, S. *Br. J. Cancer* **2010**, *102* (4), 704–709.

(58) Zheng, L.; Jia, J.; Finger, L. D.; Guo, Z.; Zer, C.; Shen, B. *Nucleic Acids Res.* **2011**, *39* (3), 781–794.

(59) Nikolova, T.; Christmann, M.; Kaina, B. *Anticancer Res.* **2009**, *29*, 2453–2459.

(60) Giacometti, a.; Cirioni, O.; Schimizzi, a. M.; Del Prete, M. S.; Barchiesi, F.; D'Errico, M. M.; Petrelli, E.; Scalise, G. *J. Clin. Microbiol.* **2000**, *38* (2), 918–922.

(61) Daghistani, H. I.; Issa, A. a.; Shehabi, A. a. *FEMS Immunol. Med. Microbiol.* **2000**, *27*, 95–98.

(62) Brandl, F. P.; Seitz, A. K.; Teßmar, J. K. V; Blunk, T.; Göpferich, A. M. *Biomaterials* **2010**, *31*, 3957–3966.

(63) Sun, J.; Jiang, G.; Qiu, T.; Wang, Y.; Zhang, K.; Ding, F. *J. Biomed. Mater. Res. - Part A* **2010**, *95* (4), 1019–1027.

(64) Williams, M. A. K.; Vincent, R. R.; Pinder, D. N.; Hemar, Y. *J. Nonnewton. Fluid Mech.* **2008**, *149* (1-3), 63–70.

(65) Mansel, B. W.; Keen, S.; Patty, P. J.; Hemar, Y.; Williams, M. A. *Rheol. - New Concepts, Appl. Methods* **2013**, *2* (1), 1–21.

(66) Zhu, Y.; Li, M.; Chen, W.; Peters, A. *J. Appl. Virol.* **2013**, *2* (1), 25–33.

(67) Irvin, J. A.; Carberry, J. R. *J. Polym. Sci., Part B Polym. Phys.* **2013**, *51* (5), 337–342.

(68) Matsukuma, D.; Yamamoto, K.; Aoyagi, T. *Langmuir* **2006**, *22* (13), 5911–5915.

(69) Cui, J.; Wang, D.; Koynov, K.; Del Campo, A. *ChemPhysChem* **2013**, *14* (13), 2932–2938.

(70) Sauerbrey, G. *Zeitschrift für Phys.* **1959**, *155* (2), 206–222.

(71) Sabot, A.; Krause, S. *Anal. Chem.* **2002**, *74* (14), 3304–3311.

(72) Kamarun, D.; Zheng, X.; Milanesi, L.; Hunter, C. A.; Krause, S. *Electrochim. Acta* **2009**, *54* (22), 4985–4990.

(73) Nguyen, M. K.; Lee, D. S. *Macromol. Biosci.* **2010**, *10*, 563–579.